The D″ Discontinuity and its Implications

Michael E. Wysession[1], Thorne Lay[2], Justin Revenaugh[2], Quentin Williams[2], Edward J. Garnero[3], Raymond Jeanloz[3], and Louise H. Kellogg[4]

A synthesis is presented of the results from over 40 different studies of a discontinuous increase in seismic velocity, referred to as the "D″ discontinuity", that occurs about 250 km above the core-mantle boundary. This discontinuity is seen in many regions around the world, both with *P* and *S* waves. The D″ discontinuity has a mean apparent depth of about 250 - 265 km for both *P* and *S* waves. While many more non-observations (where no discontinuity is observable above the seismic noise levels) exist for *P* waves than for *S* waves, both *P* and *S* non-observations and observations are distributed with little obvious geographical coherence. The D″ discontinuity is often modeled as a precipitous increase in seismic velocity of about 2.5-3.0%, though most data can accommodate a transition width of up to 50 or 75 km. The D″ discontinuity is usually modeled with lower than average velocities above the discontinuity, but the velocity gradient beneath the discontinuity has been modeled with negative, positive, or zero velocity gradients. There is a strong indication that the base of D″ displays a strong decrease in seismic velocities. There is no significant correlation between large-scale seismic velocities at the base of the mantle and (1) the occurrence or absence of a D″ discontinuity, or (2) a variation in the thickness of the observed depth of the discontinuity. Available seismic evidence leaves several possibilities open for D″ discontinuity origins. Ponding of the remnants of subducted slabs may provide a large-enough decrease in temperature to generate a 3% velocity increase. A mineralogical phase change in a major silicate constituent, perhaps caused by thermal or chemical anomalies, might provide a significant velocity increase. In both cases, a mechanism must exist to cause significant topography on the discontinuity. A third possibility is of significant heterogeneity, either as a stable chemical boundary layer or in the form of laminar layers (perhaps from core-mantle reactions or of ancient ocean crust) that are scattered about the base of the mantle.

1. INTRODUCTION

Few seismic observations have revolutionized our concept of the deep Earth like the discovery of a discontinuous increase in velocity a few hundred kilometers above the core-mantle boundary (CMB). This shattered the prevailing paradigm that reduced velocity gradients predominate at the base of the mantle, and led to further investigations of lateral heterogeneity in the D″ region, the lower 200-300 km of the mantle. The D″ discontinuity, with its variations in structure and geographical distribution, remains a vital component of any synthesis of knowledge about the CMB, and poses intriguing implications for mineral physics and geodynamical modeling of CMB boundary layer processes.

[1]Department of Earth and Planetary Sciences, Washington University, St. Louis, MO
[2]Institute of Tectonics and Earth Sciences Department, University of California, Santa Cruz, CA
[3]Department of Geology and Geophysics, University of California, Berkeley, CA
[4]Department of Geology, University of California, Davis, CA

The Core-Mantle Boundary Region
Geodynamics 28

The discovery of the D″ discontinuity modified the classic definition of D″. Many geoscientists currently use the discontinuous velocity *increase* to define the top of the D″ region, though this name was introduced by *Bullen* [1949] for the region of a *decrease* in the seismic velocity gradients at the base of the mantle, an observation made previously by *Gutenberg* [1913], *Witte* [1932], *Dahm* [1934], *Gutenberg and Richter* [1939], and *Jeffreys* [1939]. In keeping with this tradition, we will use the term "D″" to refer to the region of the base of the mantle that displays a velocity gradient less than that of the lower mantle above it (D′), and the "D″ discontinuity" as the anomalous increase in seismic velocities that is reported to occur at a depth that often but not always coincides with the top of D″. While evidence of inhomogeneous structure and decreasing velocity gradients at the base of the mantle accumulated for decades [*Cleary*, 1974], the possibility of a discontinuity with increasing velocity at the top of D″ was not suggested until the 1970's. *Mitchell and Helmberger* [1973] modeled *ScS* amplitudes and waveforms using a 4-7% *S*-velocity (V_S) increase about 40-70 km above the CMB, while a series of detailed *P*-wave apparent velocity measurements between 75° and 95° suggested the presence of a 1.5% *P*-velocity (V_P) increase about 180 km above the CMB [*Wright*, 1973; *Wright and Lyons*, 1975, 1981]. Both sets of observations were subtle and contentious; for example, many observations appear to require negative velocity gradients above the CMB rather than the strong increase proposed by *Mitchell and Helmberger* [1973], and seismic anisotropy may provide a better explanation for these data [*Lay et al.*, 1998]. The breakthrough came when *Lay and Helmberger* [1983] presented definitive evidence for a rapid 2.75% increase in V_S 250 to 300 km above the CMB, and *Wright et al.* [1985] showed waveform data supporting the existence of a 3% V_P increase 180 km above the CMB. This velocity increase has been studied in many subsequent investigations, listed in Table 1, and been the focus of several reviews [*Young and Lay*, 1987a; *Lay*, 1989, 1995; *Loper and Lay*, 1995; *Weber et al.*, 1996].

Interpretation of the D″ discontinuity in terms of mineral physics and geodynamics remains uncertain, although the seismological models provide guidance for possible thermochemical scenarios. The D″ discontinuity may involve a change in chemistry [*Bullen*, 1949], either of primordial origin, or growing from continued mantle differentiation [*Christensen and Hofmann*, 1994] and/or core-mantle reactions [*Knittle and Jeanloz*, 1989, 1991]. The D″ discontinuity may represent a transition in flow regime, deformational mechanisms, mineral alignment and/or structural fabric of the base of the mantle [e.g., *Lay et al.*, 1998]. It may be an isochemical phase change: the instability boundary for lower mantle constituents [*Stixrude and Bukowinski*, 1992]. There may also be a thermal component to it, related to the accumulation of subducted lithosphere [*Silver et al.*, 1988].

A better understanding of the geophysical processes taking place in the CMB region will require continued seismological observations of the D″ discontinuity and other properties of the lowermost mantle, such as seismic anisotropy [*Maupin*, 1994; *Vinnik et al.*, 1995; *Kendall and Silver*, 1996; *Lay et al.*, 1998], CMB scattering [*Bataille et al.*, 1990], large-scale lateral variations [*Dziewonski et al.*, 1996], and the extent of the ultra-low velocity zone (ULVZ) [*Garnero et al.*, 1998]. This paper aims to synthesize our current knowledge of the D″ discontinuity, its magnitude, depth and sharpness, the extent of its geographical distribution, and the structure above and below it. We also describe possible physical interpretations of the seismic data.

2. SEISMIC OBSERVATIONS

Abrupt velocity increases with depth produce triplications in seismic wavefields, involving three arrivals at certain distances that correspond to energy turning above the velocity increase, reflecting off of it, and turning below it. Observations of triplication arrivals and pre-critical reflections are the fundamental basis for D″ velocity models with rapid velocity increases. Arrival times of the triplication phases and their amplitudes and waveshapes provide constraints on the location and structure of the velocity increase. Usually these are measured relative to direct *P* or *S* phases or core-reflections. In some cases triplicated arrivals are directly observable on individual seismograms, though stacking of many seismograms is often required. In addition, there are many other seismic observations of structure near the base of the mantle, usually with large-scale resolution, that are compatible with, but not uniquely diagnostic of the presence of a fast velocity layer below the discontinuity. These include studies of *ScS-S* and *PcP-P* travel times and amplitudes, core-diffracted *Sdiff* and *Pdiff* waves, *PKP-AB* - *PKP-DF* times, and tomographic imaging.

2.1. Direct Observations: PdP and SdS

Detection of the D″ discontinuity involves observations of the *SdS* and *PdP* phases. Depending upon the distance travelled, these phases correspond to different wavefield interactions with the D″ discontinuity. At distances less than 70° ($\Delta < 70°$), *PdP* and *SdS* are simple (pre-critical) reflections off of the discontinuity. At greater distances *PdP* and *SdS* involve two separate phases. *Pbc* and *Sbc* reflect off of the D″ discontinuity, while *Pcd* and *Scd* turn below the discontinuity, being very dependent upon the velocity gradient within D″ (*Pab* and *Sab* are the phases that bottom above D″) (Figure 1). Before the cross-over distance of 82° (for a 600 km deep earthquake), the phases *Scd* and *Sbc* both arrive between *S* and ScS. For most distances less than the cross-over point *Sbc* and *Scd* arrive too close in time to be distinguished from each other, and appear as a single arrival. At greater distances *Sbc* and *Scd* become increasingly separated. Most studies use observations of the composite *PdP* or *SdS* phases at Δ = 65°-80° [e.g., *Lay et al.*, 1997; *Kendall and Shearer*, 1994; *Weber*, 1993]. However, studies of the pre-critical extension of the *Pbc* or *Sbc* branch are

Table 1. List of studies identifying a discontinuous velocity increase at the base of the mantle.

Reference	Location	δlnV (%)	Height above CMB (km)	dV/dz	Data Type	Dist. (deg)	Comments
Baumgardt [1989]	Arctic Sea	2.75	344		Pcd	72-87	Variable depth on discontinuity
Ding & Helmberger [1997]	Central America	3	200	N	Scd	70-96	No P discontinuity
Gaherty and Lay [1992]	E. Siberia	2.75	290	N	Scd	65-95	SGLE fits 80% of data.
Garnero et al. [1988]	Mid Pacific	2	280	N	S-SKS-SKKS	84-94	Disc. disappears laterally
Garnero et al. [1993]	Mid-Pacific	2.4	180	N	Scd	73-82	Model SGHP
	Western Pacific	2.75	280	N	Scd	73-82	Fits models SYL1
Garnero & Lay [1997]	Alaska	*	250-275	N	Scd	45-105	Thick D" correlates with stronger anisotropy
	E. Siberia		225-250	N			
	* (SHcd increase - 2-3%; SVcd increase - 0.5-2%)						
Houard & Nataf [1992]	Franz Josef Land		300		PdP	76-88	
Houard & Nataf [1993]	NW Siberia	2.8-3	250-300		Pcd	75-82	Regional topography on disc.
Kendall & Shearer [1994]	N. Central Asia	2.75	140-370	N	Scd	63-74	Mean = 270 from 19 obs
	Alaska	2.75	160-375	N	Scd	63-74	Mean = 296 from 16 obs (Aleutians: 375 from 6 obs)
	Arctic	2.75	170-330	N	Scd	63-74	Mean = 268 from 20 obs
	Australasia	2.75	100-430	N	Scd	63-74	Mean = 245 from 27 obs (E. Austral.: 300 from 5 obs)
Kendall & Nangini [1996]	Carib. (10N,60-85W)	2.75	250	N	Scd	73-99	Models SKNA1, SKNA2
	Carib. (20N,80-90W)	2.45	290	0	Scd	73-99	No disc. at 25°N, 65-80°W
Krüger et al. [1993]	Severnaya Zem.	0.5-2.	131-178		PdP DB	67-68	Large vars. over short distances
Krüger et al. [1995]	North Pole	1-2	200		PdP DB	84	
	Svalbard	1-2	260		PdP DB	69-70	
	Baffin Island	1-2	180		PdP DB	82	
	Foxe Basin	1-2	260		PdP DB	73	
Lay & Helmberger [1983]	Alaska	2.75	280	0,P	SdS	70-95	Model SLHO
	Caribbean	2.75	253	0,P	SdS		Model SLHA
	NW Siberia	2.75	320	0,P	SdS		Model SLHE
Lay & Young [1991]	Alaska	2.1	175		S+Sdiff	70-105	Both SH and SV are modeled
Lay et al. [1997a]	Eurasia, Alaska		200-300	N	Scd	65-95	ΔVs of ±4% in top 50 km of D" and/or disc. topogr. of ± 50 km
Matzel et al. [1996]	Alaska	3.0	291	N	SH (Scd)	70-106	SV flat, no discontinuity
Mitchell & Helmberger [1973]	Caribbean, Alaska	4-7	40-70		ScS/S	60-75	From ScS/S amps., ScS-S times
Nataf & Houard [1993]					binned p	70-98	Global feature
Nataf & Breger [1996]	Gulf of Alaska	3	300		Pbc stack	24	Δρ = +3%, disc thickness ≤ 8 km
Neuberg & Wahr [1991]	Tasman Sea		none		Pbc	35	No D" discontinuity
	NE Australia		320		Pcd stack	70	
Olivieri et al. [1997]	Antarctic plate	3	315	N	SdS	66-82	No disc. at a nearby spot
Revenaugh & Jordan [1991b]	NW, W, SW Pacific	2.75	270-340		ScSn stack		Disc. seen in 7 regions, but not in 6 others; ρ increase of 1.7%
Scherbaum et al. [1997]	Novaya Zem.		389		PdP	68	Correlation of thin D" with fast D" Vp
	Severnaya Zem.		139		PdP	68	
Schimmel & Paulssen [1996]	S. Fiji Basin		180		Sbc stack	13-26	D" topography of ± 30-50 km with λ = 1200-1600 km
Shibutani et al. [1993]	Western Pacific	1.1-1.6	289	P	PdP	67-83	No discontinuity observed for a spot beneath the N. Pacific
Thomas & Weber [1997]	Nansen, NE Siberia	3	286-293		Pcd	60-100	D" topography of 10-100 km with λ = 400 - 1200 km
Valenzuela&Wysession [1997]	NE Siberia	4.6	210	N	SHdiff	95-102	
	ECentral Pacific	3.4	185	N	SHdiff	105-120	

Table 1. List of studies identifying a discontinuous velocity increase at the base of the mantle.

Reference	Location	δlnV (%)	Height above CMB (km)	dV/dz	Data Type	Dist. (deg)	Comments
Vidale & Benz [1993a]	Northern Pacific	0			ScP,PcP stack	36-48	No discontinuity
Vidale & Benz [1993b]	Arctic Sea	1.5	130	0	Pcd stack	92-103	
Weber & Davis [1990]	NW Siberia	3	293	P	PdP	73-80	Models PWDK, SWDK
		2	293	P	SdS		
Weber [1993]	Nansen Basin	3	279	P	Pcd	74-79	Only 74 of 255 high S/N events show Pcd
	Kara Sea, NW Siberia	3	286	P	Pcd		
	NW Siberia	2.3-2.6	281-316	0,P	Scd		No Scd at Nansen B. + Kara Sea
Weber & Körnig [1992]	North Atlantic Ridge	2-3	250		Pcd (ISC)	70-80	Eight distinct regions found with little evidence of Pcd
	NCentral Siberia	2-3	230		Pcd (ISC)	70-80	
	Japan	2-3	180		Pcd (ISC)	70-80	
	central Mid-Atlantic	2-3	260,310		Pcd (ISC)	70-80	
	Ecuador coast	2-3	340		Pcd (ISC)	70-80	
Weber [1994]	Northern Siberia	3	205		Pcd	74-79	Thin fast layer, perhaps lamellar
Wright et al. [1985]	Indonesia, Pacific	2.8	163	N	Pcd	78-92	
Yamada & Nakanishi [1996]	Micronesia		170		PdP stack	~65-70	
Young & Lay [1987b]	India	2.75	280	N	Scd	75-100	SYL1, λ = 1200 - 1600 km
Young & Lay [1990]	Alaska	2.75	243	N	Scd	60-100	SYLO, λ of var. is < 500 km

made at shorter distances [*Schimmel and Paulssen*, 1996; *L. Breger and H.-C. Nataf*, personal communication], and of the *Pcd* branch alone at great distances [*Vidale and Benz*, 1993b]. Energy diffracted around the D″ discontinuity at Δ > 100°, predicted by *Schlittenhardt* [1986], has also been observed [i.e., *Kendall and Nangini*, 1996]. Table 1 includes the distances of data used.

Figure 2 shows an example of *SdS* data and synthetics generated using the model SYLO. Note that at the greater distances *SdS* appears as an extended shoulder of the *S* arrival, but is a distinct phase at closer distances. The clear *SdS* arrivals (mostly *Scd* energy) allow individual records to be analyzed, either through modeling with synthetic seismograms [*Lay and Helmberger*, 1983; *Young and Lay*, 1987b; *Young and Lay*, 1990; *Gaherty and Lay*, 1992; *Garnero et al.*, 1993; *Matzel et al.*, 1996; *Ding and Helmberger*, 1997], through a phase-stripping technique to remove the *S* and *ScS* phases [*Kendall and Shearer*, 1994; *Kendall and Shearer*, 1995], or through a combination of both [*Kendall and Nangini*, 1996]. While most *SdS* studies use energy at periods greater than 10 s, most *PdP* studies are done at periods of about 1 s where *PdP* is often below noise levels. Stacking techniques using array data enhance the *PdP* signal [*Weber and Davis*, 1990; *Yamada and Nakanishi*, 1996; *Houard and Nataf*, 1992; *Weber*, 1993; *Vidale and Benz*, 1993a,b]. *PdP* arrivals are identified on vespagrams, that stack a set of array records at different ray parameters. An example is shown in Figure 3 from *Weber et al.* [1996]. Another form of stacking is the double beam method [*Krüger et al.*, 1993, 1995, 1996; *Sherbaum et al.*, 1997; *Thomas and Weber*, 1997], where records are combined from both seismometer arrays (e.g., the Gräfenberg or NORSAR arrays) and source arrays (e.g., nuclear tests in Nevada and Russia).

There are very few other types of seismic data that are able to resolve a D″ discontinuity. *Revenaugh and Jordan* [1991b] stack long-period multiple-*ScS* reverberations to enhance *SdS* and quantify the impedance contrast across the discontinuity, finding a density increase of 1.7% for an assumed V_S increase of 2.75%. *Valenzuela and Wysession* [1997] use azimuthal profiles of core-diffracted *Pdiff* and *Sdiff* waves in two ways: (1) *Pdiff* and *Sdiff* travel time slownesses vary as functions of frequency because they sample the lowermost mantle at different depths, and so are sensitive to a D″ discontinuity, and (2) the amplitude decrease of *Sdiff* as a function of frequency is indicative of radial structure, resolving a D″ discontinuity in two CMB regions.

2.2. Indirect Seismic Evidence

A velocity increase of 2-3% atop D″ is large enough that, even given the lower-than-average velocities above the D″ discontinuity found in many models, the net effect can still be a substantial increase in average lower mantle velocity relative to standard reference models. Many studies lacking the resolution to detect the discontinuity have identified heterogeneous regions of fast seismic velocities at the base of the mantle. Globally averaged models suggest that average D″ velocities are less than expected for a projection of adiabatic gradients from the rest of the lower mantle (region D′). This is seen in studies of normal modes [*Kumagai et al.*,

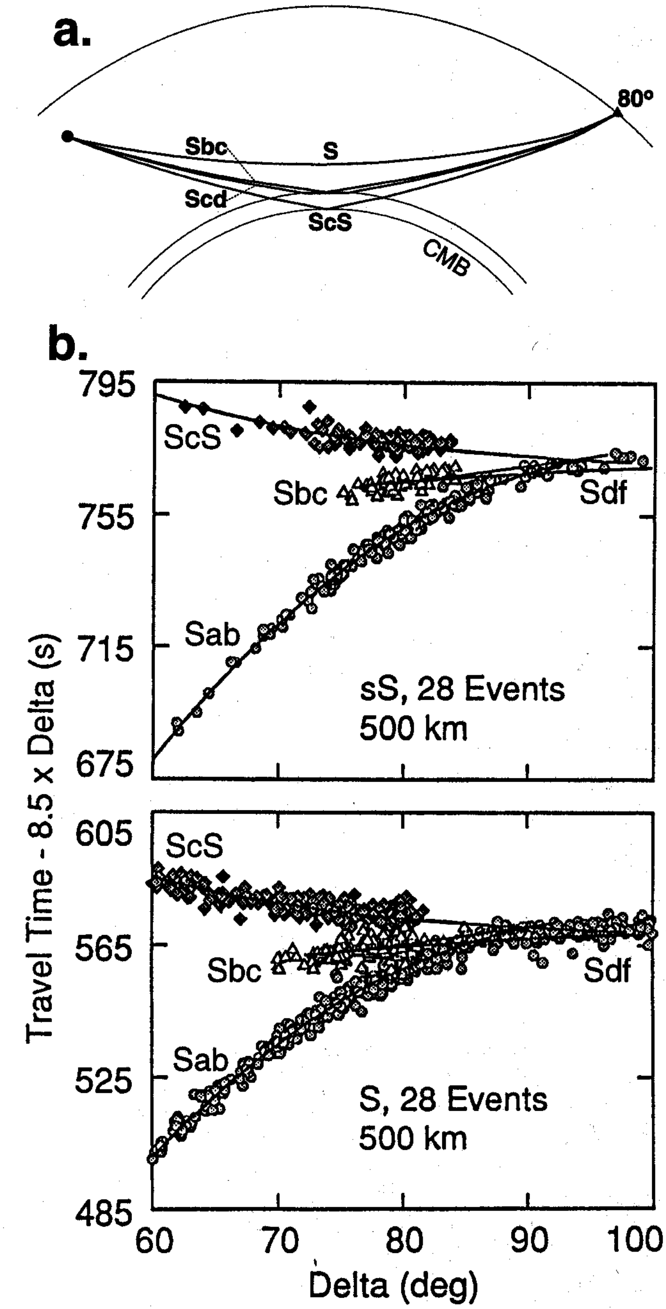

Figure 1. (a) The geometrical paths of the *ScS* precursors, *Sbc* and *Scd*, that result from a discontinuous increase in seismic velocity about 250 km above the core-mantle boundary. Shown here for an earthquake-station distance of 80°, the *Sbc* phase is a reflection off of the "D″ discontinuity", while the *Scd* phase is a refraction just below the discontinuity. An analogous situation occurs for the *PcP* precursors *Pbc* and *Pcd*. The two phases are indistinguishable at large distances and are often referred to together as *SdS* (or *PdP*). (b) An example from *Young and Lay* [1990], showing the different travel time curves for the arrivals of *S* (circles), *SdS* (triangles), and *ScS* (diamonds). The data are from Kuril, Japan and Izu-Bonin earthquakes, converted to a common source depth of 500 km.

1992], and travel times [*Kennett et al.*, 1995], as well as models that combine several seismic data sets like PREM [*Dziewonski and Anderson*, 1981]. Yet, anomalously fast regions of D″are found in studies of the travel times of *ScS* [*e.g.*, *Lavely et al.*, 1986; *Woodward and Masters*, 1991; *Wysession et al.*, 1994], *PcP* [*Zhu and Wysession*, 1997], *PKP* [*Creager and Jordan*, 1986; *Song and Helmberger*, 1993; *McSweeney and Creager*, 1994; *Sylvander and Souriau*, 1996], *Sdiff* and *Pdiff* [*Wysession et al.*, 1992; *Souriau and Poupinet*, 1994; *Wysession*, 1996a; *Valenzuela and Wysession*, 1997; *Kuo and Wu*, 1997], and combinations of phases in tomographic inversions [*Inoue et al.*, 1990; *Tanimoto*, 1990; *Pulliam et al.*, 1993; *Su et al.*, 1994; *Vasco et al.*, 1994; *Masters et al.*, 1996; *Dziewonski et al.*, 1996; *Li and Romanowicz*, 1996; *Grand et al.*, 1997, *van der Hilst et al.*, 1997]. The variations found by these studies can exceed a 3% increase in average D″ velocity relative to reference earth models, and so are compatible with models of a D″ discontinuity. An attempt to correlate the locations of the turning points of observed *PdP* and *SdS* phases with some of these velocity models will be discussed later.

3. STRUCTURE OF VELOCITY MODELS

While models of the D″ discontinuity show a large degree of variability, they tend to have many characteristics in common. Several models for *S*-velocity structures are shown in Figure 4, and many others are described in Table 1. Most models are variations of the original SLHO model of *Lay and Helmberger* [1983], which had a 2.75% discontinuous increase in V_S 280 km above the CMB, with lower-than-average velocities above the discontinuity. The latter feature is not resolved by the data, but is an artifact of embedding the discontinuity in a smooth reference model. If there is no velocity reduction the discontinuity must be placed about 20 km deeper. Studies of *SdS* and *PdP* provide better resolution of the top of D″ than of the bottom. Models are found through non-unique forward-modeling, and trade-offs exist between model parameters [*Young and Lay*, 1987b]. In matching *SdS* and *PdP* data with synthetics, trade-offs exist between the depth and magnitude of the discontinuity for travel times, and between the magnitude and sharpness of the discontinuity for amplitudes. However, support for these models is strong because of their ability to match both the times and amplitudes of *PdP* and *SdS* data for $\Delta = 65° - 100°$, and of *Pdiff* and *Sdiff* for $\Delta > 100°$.

3.1. *Magnitude of the Discontinuity*

The magnitude of the D″ discontinuity ranges from about zero (in places where no discontinuity can be resolved) to about 3%, for both V_P and V_S. A small velocity increase would not be detected above noise levels, but studies with good resolution find regions with no evidence of a discontinuity. *Krüger et al.* [1995] find regions with less than a 0.5% possible V_P increase, if the discontinuity is

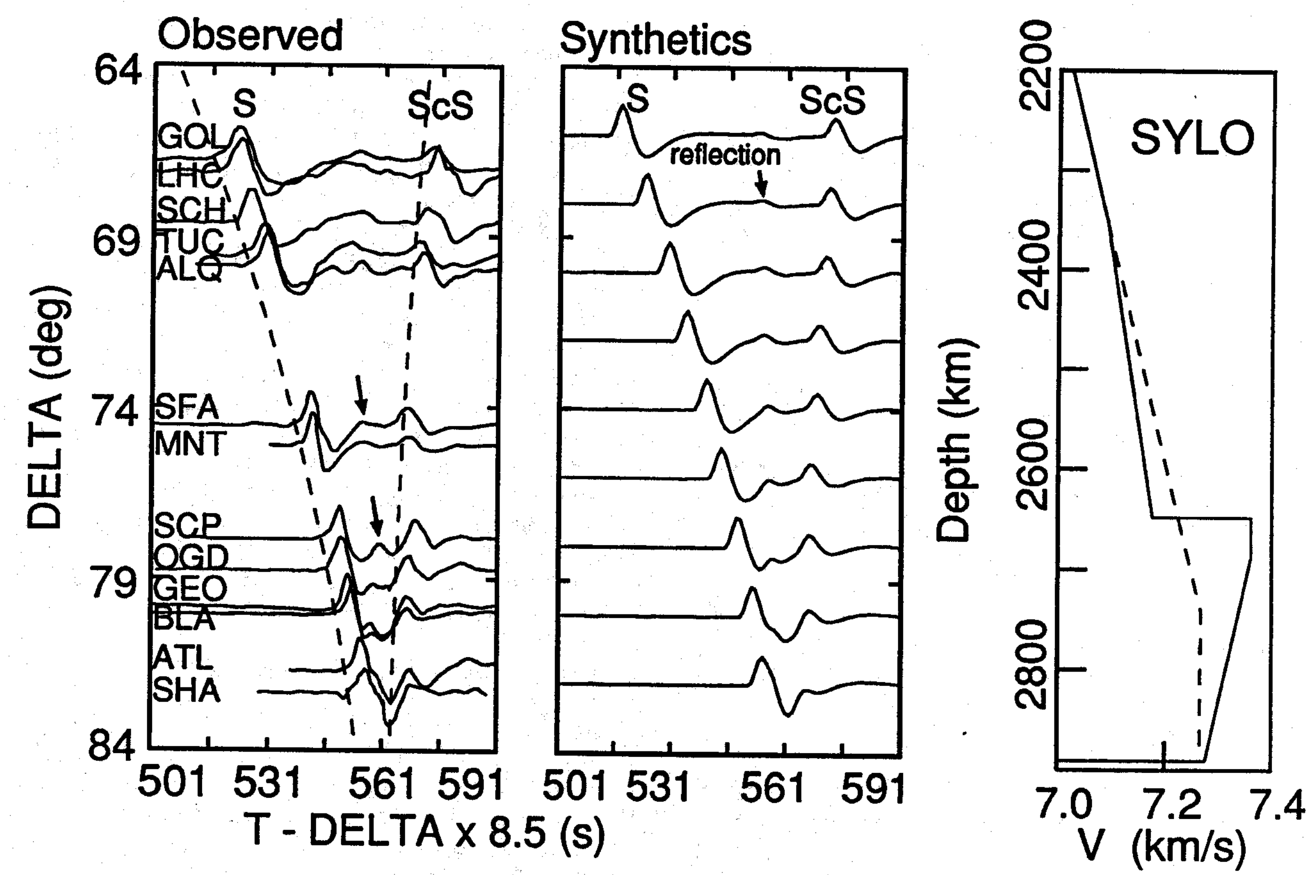

Figure 2. An example showing the forward modeling of *Scd* data for a 9/05/70 earthquake in the Kuril Arc recorded in the United States. The data (left) show a small phase (*Scd*) that arrives in between the *S* and *ScS* arrivals, and is well predicted by the synthetic seismograms (middle) created by the SYLO *S*-velocity model for the base of the mantle (right).

sharp. *Ding and Helmberger* [1997] find no V_P increase beneath Central America to within 1%, and the waveform analyses of *Lay et al.* [1997] find non-observations where the maximum possible undetected increase is 1.5%.

Velocity increases of 2.5-3.0% are consistent with most studies of *SdS* [*Lay and Helmberger*, 1983; *Young and Lay*, 1987; *Young and Lay*, 1990; *Gaherty and Lay*, 1992; *Garnero et al.*, 1993; *Kendall and Shearer*, 1994; *Kendall and Nangini*, 1996; *Matzel et al.*, 1996; *Ding and Helmberger*, 1997; *Garnero and Lay*, 1997; *Lay et al.*, 1997; *Valenzuela and Wysession*, 1997] and *PdP* [*Wright et al.*, 1985; *Baumgardt*, 1989; *Weber and Davis*, 1990; *Weber and Körnig*, 1992; *Houard and Nataf*, 1993; *Weber*, 1993, 1994]. There are also models of lesser V_P increases [1.5%, *Vidale and Benz*, 1993b; 0.7-1.5%, *Krüger et al.*, 1993; 0.5-2.0%, *Krüger et al.*, 1995], and of lesser V_S increases [2.1%, *Lay and Young*, 1991]. Studies of both *PdP* and *SdS* using similar earthquake-station geometries and analysis techniques have found V_P and V_S increases to differ, but not consistently. *Weber* [1993] found regions of D″ beneath the Nansen Basin and Kara Sea with a 3% V_P increase and none for V_S, and a region of D″ beneath NW Siberia with a 2.3-2.6% V_S increase and none for V_P.

There may be a connection between observations of transverse isotropy at the base of the mantle and the differences between V_{SH} and V_{SV} discontinuities. Observed transverse isotropy in D″ usually (but not always) takes the form of slower V_{SV} relative to V_{SH} (see *Kendall and Silver* [1996], and *Lay et al.*, [1998]), and the magnitudes of V_{SV} discontinuities maybe less than those of V_{SH}. *Garnero and Lay* [1997] found discontinuous V_{SH} increases of 2-3% from *SHcd*, but only 0.5-2% V_{SV} increases for *SVcd* in a region beneath Alaska. Using *SHcd* and *SVcd* also beneath Alaska, *Matzel et al.* [1996] found a 3% V_{SH} increase but no discernible V_{SV} increase. In examinations of *SVdiff*, *Vinnik et al.* [1995] postulate a discontinuous *decrease* in V_S 220 km above the CMB beneath the central Pacific, with the V_{SV} discontinuity is more negative than for V_{SH}. A few observations do report V_{SV} greater than V_{SH} [*Lay et al.*, 1998].

The similarity of the magnitudes of the V_S and V_P discontinuities (about 2.5-3.0) is very unusual, given that V_S variations in D″ tend to be greater than V_P variations by about a factor of 4 [*Robertson and Woodhouse*, 1996; *Bolton and Masters*, 1996; *Grand et al.*, 1997]. This result becomes even more extreme when considering that most *SdS* observations are of *SH* waves, and because the *SV* velocities are generally less than for *SH*, the net effect would be that the isotropically-averaged V_S discontinuity increases would actually be less than for V_P. A caveat should be noted that the threshold for observing *PdP* and *SdS* varies greatly between different studies, and a direct comparison may not be valid. For instance, Table 2 lists the results of several comparisons involving observations and non-observations of the D″ discontinuity (discussed in detail in a later section). It is suggested that *PdP* non-observations (where a discontinuity was below the threshold of the noise level) represent a greater percentage of the total *P* data set than *SdS* non-observations do for the *S* data (further discussed below). The implication is that the mean V_P discontinuity magnitude may actually be less than for V_S. But in any case, there is a strong suggestion that the mechanism for the D″ discontinuity is not the same as the mechanisms for the large-scale lateral velocity variations at the CMB.

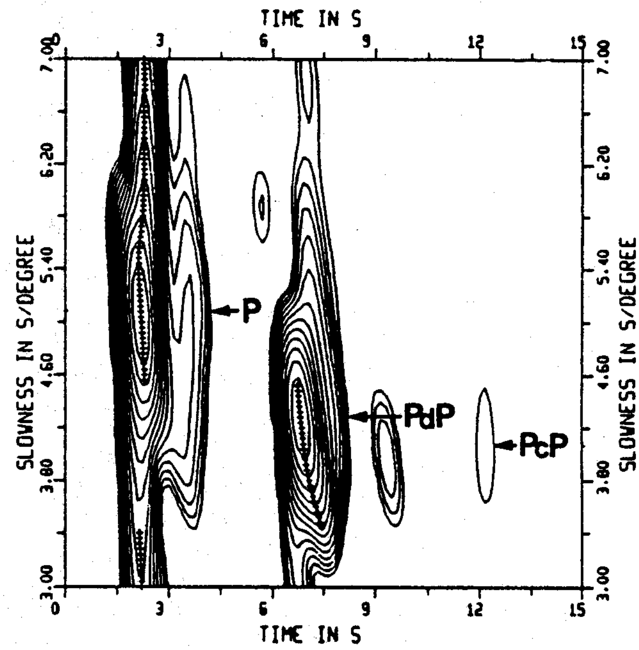

Figure 3. Figure from *Weber et al.* [1996] showing a vespagram for a Kuril earthquake recorded at the Gräfenberg (GRF) Array in Germany. This stacking procedure provides the difference between both slowness and time of the *P* and *PdP* arrivals, which can be converted into the depth of the D″ discontinuity. The *PdP* arrival is actually much stronger than the *PcP* arrival at the distances of these seismograms (about 75°-79°).

3.2. Sharpness of the Discontinuity

Using near-vertical *PdP* reflections off of the top of D″, *L. Breger and H.-C. Nataf* [personal communication] were able constrain the width of the D″ discontinuity transition to be less than 8 km in one location. The *PdP* arrivals had a dominant period of 2.5 s, as compared to a *PcP* dominant period of 1 s. While this suggests that the D″ discontinuity is not as sharp as the CMB, it does limit the width to being not much greater than $\lambda/4$, or 8 km [*Richards*, 1972]. The effects of topography and 3D scattering on this estimate of thickness have not been fully investigated. Long-period *SdS* arrivals cannot constrain the width of the transition, as a velocity increase distributed over about 100 km in depth matches the data as well as a sharp discontinuity [*Young and Lay*, 1987b; *Gaherty and Lay*, 1992; *Garnero et al.*, 1993]. However, a gradual transition greatly decreases pre-critical short-period *PdP* amplitudes [*Young and Lay*, 1987b], placing a maximum transition thickness limit at ≈ 75 km [*Weber et al.*, 1996]. *Revenaugh and Jordan* [1991a,b], using the reflection coefficients of multiple *ScS* bounces, limit the width of the transition to be ≈ 50 km, and modeling of broadband *SdS* signals under Alaska indicates a transition zone width of ≤ 30 km [*Lay and Young*, 1990].

3.3 Velocity Gradients

As seen in Figure 4, models often show a decrease in velocity from reference model values in the regions above the D″ discontinuity, though *Ding and Helmberger* [1997] and *Kendall and Nangini* [1996] model structure under the Caribbean with no velocity reduction above the discontinuity. Below the discontinuity, however, the models differ significantly. Some have a zero or slightly positive gradient, like SLHO, SLHA, SLHE [*Lay and Helmberger*, 1983], PWDK, SWDK [*Weber and Davis*, 1990], and SKNA2 [*Kendall and Nangini*, 1996]. Others have a strong negative gradient, like SYL1 [*Young and Lay*, 1987b], SGHE [*Garnero et al.*, 1988], and SKNA1 [*Kendall and Nangini*, 1996]. The models of *Valenzuela and Wysession* [1997] and *Ritsema et al.* [1997] use the waveforms of core-diffracted waves, sensitive to the gradients within D″, finding strong negative gradients just above the CMB in the regions examined. Still other models have a zero gradient at the top of D″ with a negative gradient below, like SYLO [*Young and Lay*, 1990], SGLE [*Gaherty and Lay*, 1992], and SGHP [*Garnero et al.*, 1993]. Because the rate of velocity decrease above the discontinuity can vary, the effect on travel times of phases like *ScS* and *PKP* differ. Models like SGHP (Pacific) and SYL1 (Indian Ocean) are on average slower than PREM, even including the discontinuity. Others like SGLE (Eurasia) and SYLO (Alaska) have faster-than-average velocities. *SdS* and *PdP* arrivals do not require the existence of faster-than-average velocities, but may involve structure superimposed upon both positive and negative anomalies.

A velocity model that is significantly different from others is LAM+ [*Weber*, 1994], that consists of a narrow zone (20 km thick) of very fast velocities atop D″. This provides waveforms very similar to conventional models at $\Delta \leq 85°$, but not the secondary arrivals observed beyond about 85°.

4. GEOGRAPHICAL ANALYSIS

Figures 5 and 6, Plates 1 and 2 and Table 2 show a synthesis of studies of the D″ discontinuity, including correlations between observations and non-observations, observations with average D″ velocities, correlations between *P* and *S* wave studies, etc. The results are presented with the caveat that studies of many types of data with many different techniques are incorporated. They differ in age, and may differ in quality. For the sake of manageability, all available studies were grouped within Table 2 into 5 different sets of discontinuity *observations* (S16, KSN, LGYG, P40, WK) and *non-observations* (NoS9, NoKSN, NoLGYG, NoP67, NoWK), with the inevitable result of comparing apples and oranges. For instance, the KSN set combines 147 geographically binned values from *Kendall and Shearer* [1994], which are based on 217 individual seismograms, with 65 individual data from *Kendall and Nangini* [1996]. LGYG is mostly individual waveforms from the compilation of *Lay et al.* [1997], but includes the multi-waveform discontinuity determinations of *Garnero et al.* [1993]. The discontinuity data in S16 and P40 are the results of analyses of large numbers of waveforms (*e.g., Vidale and Benz* [1993*a,b*] used over 1000), but the number and geographical extent of the data vary. Nevertheless, some interesting results emerge.

4.1. Observations and Non-Observations

Plates 1 and 2 show the geographical distribution of locations of observed D″ discontinuities for V_P and V_S, as well as locations where a discontinuity could not be observed. These non-observations are where signal is below noise level, and do not exclude the possibility of small discontinuities or of distributed transition zones that are weak reflectors of short period signals. D″ discontinuities are observed in many parts of the globe, and there has been much discussion about the possibility of it being a global feature [*Nataf and Houard*, 1993]. If the discontinuity is global, then other mechanisms such as topography are required to explain the many non-observations. It is difficult to determine the confidence level of regions that consistently show the presence or absence of a discontinuity, as different studies have differing resolutions, document non-observations to differing degrees, and use different quality data. However, some D″ regions like Franz Josef Land (Arctic Sea) show consistent observations for both V_P and V_S, and some like NE Canada and Greenland show consistent non-observations (data mostly from *Krüger et al.* [1995]).

Estimates for the lateral extent of coherent D″ reflectors vary greatly, with regions as small as a few hundred kilometers [*Weber*, 1994] and as large as 1500 km [*Young and Lay*, 1990] being characterized with relatively uniform structure. The nature of lateral transitions in the discontinuity structure is unknown: the fast layer may pinch out, or the discontinuity may fade laterally.

An interesting observation in Table 2 is the difference between the KSN and LGYG sets of the ratios of observations to non-observations (212/179 for KSN/NoKSN, and 508/61

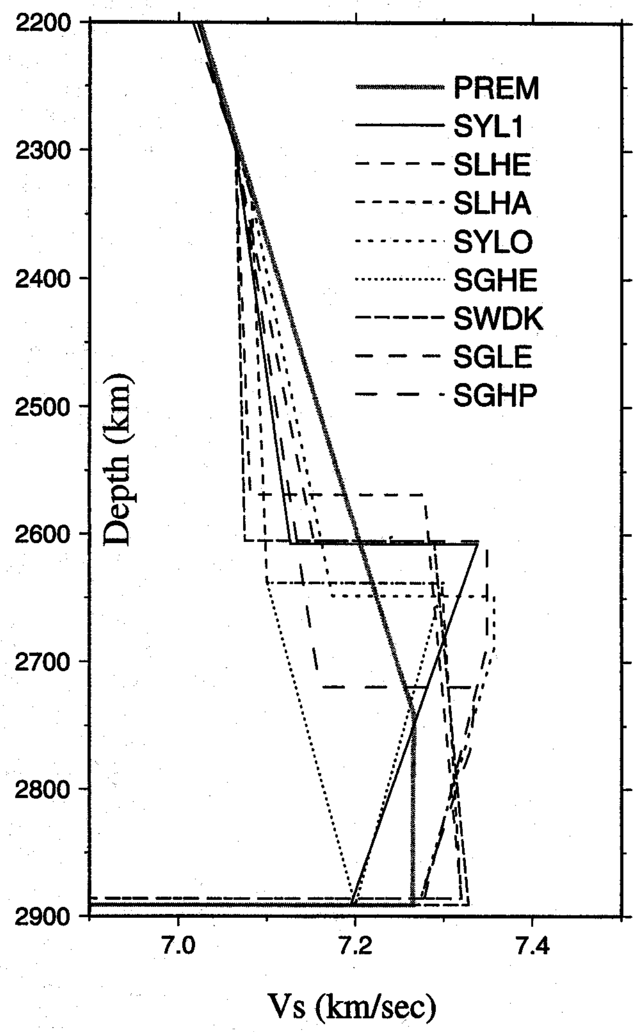

Figure 4. An example of eight variations of shear velocity models for the base of the mantle displaying the D″ discontinuity. These models are all roughly similar in that they have about a 2.5-3.0% discontinuous velocity increase, but differ in several ways including the depth of the discontinuity, the gradient below the discontinuity, the degree to which velocities are decreased above the discontinuity, and the mean vertical velocity. Several other models (not shown) represent the discontinuity as a gradual transition over 50-120 km. The range of models is similar for *P* velocities. The models shown are SLHA and SLHE [*Lay and Helmberger*, 1983], SYL1 [*Young and Lay*, 1987b], SGHE [*Garnero et al.*, 1988], SYLO [*Young and Lay*, 1990], SWDK [*Weber and Davis*, 1990], SGLE [*Gaherty and Lay*, 1992], and SGHP [*Garnero et al.*, 1993]. Model PREM [*Dziewonski and Anderson*, 1981] is also shown.

Table 2. Analysis of data sets revealing a velocity increase at the base of the mantle.

Obs. Type	Data Source	# of Data	Mean $\pm 1\sigma$	*Grand et al.* [1997] V_S vs. discontinuity Ave ΔV_S (%)	R[a]	*Dziewonski et al.* [1996] V_S vs. discontinuity Ave ΔV_S (%)	R[a]	*Van der Hilst et al.* [1997] V_P vs. discontinuity Ave ΔV_S (%)	R[a]	*Wysession* [1996] V_P vs. discontinuity Ave ΔV_S (%)	R[a]
S	S16[b]	16	257 ± 50	0.80 ± 0.59	0.49	1.34 ± 1.40	0.66	-0.02 ± 0.28	-0.08	-0.32 ± 0.51	-0.45
No S	NoS9[c]	9	---	0.85 ± 0.51	---	1.39 ± 1.13	---	0.07 ± 0.41	---	-0.09 ± 0.64	---
S	KSN[d]	212	251 ± 67	0.58 ± 0.87	0.04	0.44 ± 0.82	0.10	-0.01 ± 0.29	-0.01	-0.10 ± 0.44	-0.10
No S	NoKSN[d]	179	---	0.50 ± 0.94	---	0.69 ± 0.82	---	-0.01 ± 0.30	---	-0.02 ± 0.46	---
S	LGYG[e]	508	258 ± 23	0.93 ± 0.63	0.40	0.87 ± 0.88	0.37	-0.07 ± 0.32	0.56	-0.12 ± 0.51	0.01
No S	NoLGYG[e]	61	---	0.89 ± 0.42	---	0.83 ± 0.86	---	0.05 ± 0.31	---	0.02 ± 0.55	---
P	P40[f]	40	265 ± 56	0.86 ± 0.79	-0.04	1.26 ± 1.13	0.41	0.07 ± 0.50	0.09	-0.12 ± 0.57	-0.14
No P	NoP67[g]	67	---	0.64 ± 0.69	---	1.36 ± 1.31	---	0.07 ± 0.41	---	-0.09 ± 0.64	---
P	WK[h]	120	252 ± 35	0.86 ± 0.78	0.01	0.90 ± 0.87	-0.09	0.09 ± 0.28	0.13	-0.06 ± 0.42	-0.00
No P	NoWK[h]	398	---	0.38 ± 0.99	---	0.71 ± 0.66	---	0.02 ± 0.30	---	-0.03 ± 0.38	---

[a] Correlation Coefficient, R, is between the thickness of the discontinuity and the model velocity at the location of the discontinuity.
[b] Includes data from DH97, VW97, W93, SP96, WD90, and OPM97.
[c] Includes data from WD90, W93, and OPM97.
[d] Includes data from KS94 and KN96.
[e] Includes data from LGYG97 and GHG93. Discontinuity depths had 5 possible values: 243 km beneath Alaska, 286 km beneath Eurasia, 283 km beneath the Indian Ocean, 280 km beneath the west Pacific, and 180 beneath the mid-Pacific.
[f] Includes data from HN92, HN93, YN96a,b, NH91, NB96, VB93b, W93, WD90, TW97, KWSS93, KWSS95, SKW97, and STKH93.
[g] Includes data from WD90, NW91, VB93a, W93, KWSS95, DH97, and STKH93.
[h] Includes data from WK90, WK92.

for LGYG/NoLGYG). KSN is dominated by the global study of *Kendall and Shearer* [1994], while LGYG is dominated by sub-Eurasian and sub-Alaskan regional studies. While the particular numbers are not meaningful because of the inclusion of binned data (see above), the ratio for the globally-oriented KSN is about equal to 1, while the more regional LGYG ratio is close to 10. This is likely a result of differences in analysis, as KSN studies use a phase-stripping technique with long-period GDSN data while LGYG studies use synthetic waveform modeling with intermediate-period WWSSN data. The sub-Eurasian and sub-Alaskan regions examined by *Lay et al.* [1997] (and preceding studies) may also be significantly different than the global norm.

4.2. Variations in the Depth of the Discontinuity

Figures 5*a,b* show the distribution of D″ V_P and V_S thicknesses, as determined by the distance from the CMB to the D″ discontinuity. The size of the symbols are scaled to the thickness. Table 2 shows that mean thicknesses are in the range of 250 - 265 km, but scatter is large, and the means have 1σ standard deviations of about 50 km. Almost all studies of *SdS* and *PdP* have observed a variable depth of the discontinuity. The range of thicknesses was 100 - 440 km for *Kendall and Shearer* [1994]. *Lay et al.* [1997] found that $\pm$ 50 km of topography could exist over lateral distances of 200-500 km or less beneath Alaska, even in regions that showed generally stable discontinuity structure over 1500-2000 km lengths. *Thomas and Weber* [1997] found topography of 10-100 km over distances of 400-1200 km. *Kendall and Shearer* [1995] identified coherent topography variations over long distances beneath the southwest Pacific. *Schimmel and Paulssen* [1996] found that topography of $\pm$ 30-50 km over scale lengths of 1200-1600 km explained the large variation in *SdS* reflection amplitudes at short distances. This focussing-defocussing mechanism may explain alternations of observations and non-observations, even in the case of a global discontinuity.

4.3. Correlations with Averaged Lowermost Mantle Velocities

A natural question is whether the locations of the D″ discontinuity observations and non-observations correlate with large-scale models of lowermost mantle velocities. The velocity variations of these models are often attributed to

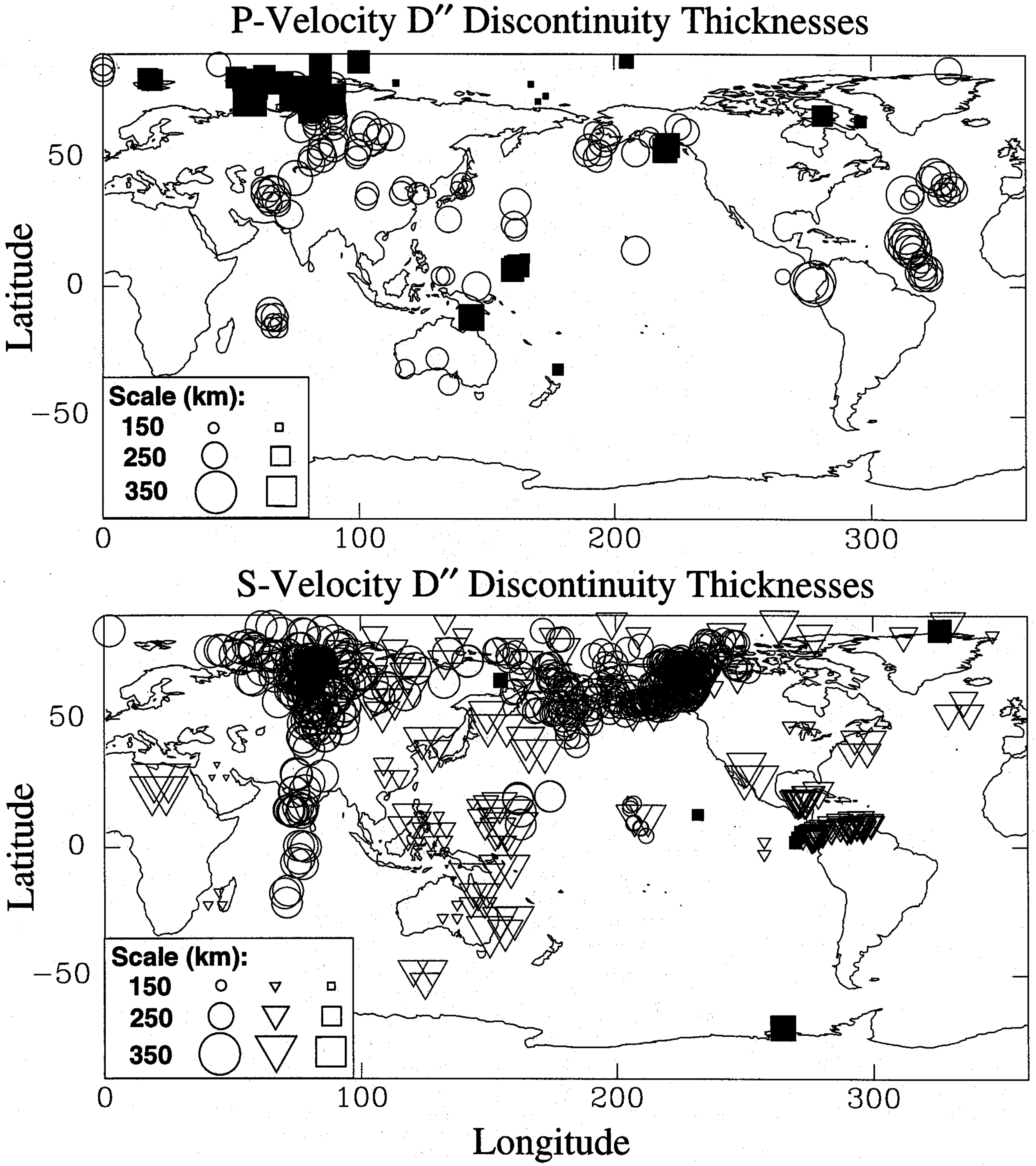

Figure 5. (Top) The geographical distribution of the inferred thickness of the D″ discontinuity for *P* velocities. Circles are for the ISC data of *Weber and Körnig* [1990, 1992], and squares are for the waveform studies of *Weber and Davis* [1990], *Neuberg and Wahr* [1991], *Houard and Nataf* [1992, 1993], *Weber* [1993], *Vidale and Benz* [1993b], *Krüger et al.* [1993, 1995], *L. Breger and H.-C. Nataf* [personal communication], *Yamada and Nakanishi* [1996], *Ding and Helmberger* [1997], *Thomas and Weber* [1997], and *Sherbaum et al.* [1997]. (Bottom) The geographical distribution of the inferred thickness of the D″ discontinuity for *S* velocities. Circles are for the waveform data of *Lay and Helmberger* [1983], *Young and Lay* [1987b], *Young and Lay* [1990], *Gaherty and Lay* [1992], *Garnero et al.* [1993], and *Lay et al.*, [1997], triangles are for the waveform data of *Kendall and Shearer* [1994] and *Kendall and Nangini* [1996], and squares are for the waveform studies of *Weber and Davis* [1990], *Weber* [1993], *Schimmel and Paulssen* [1996], *Ding and Helmberger* [1997], *Valenzuela and Wysession* [1997], and *Olivieri et al.* [1997].

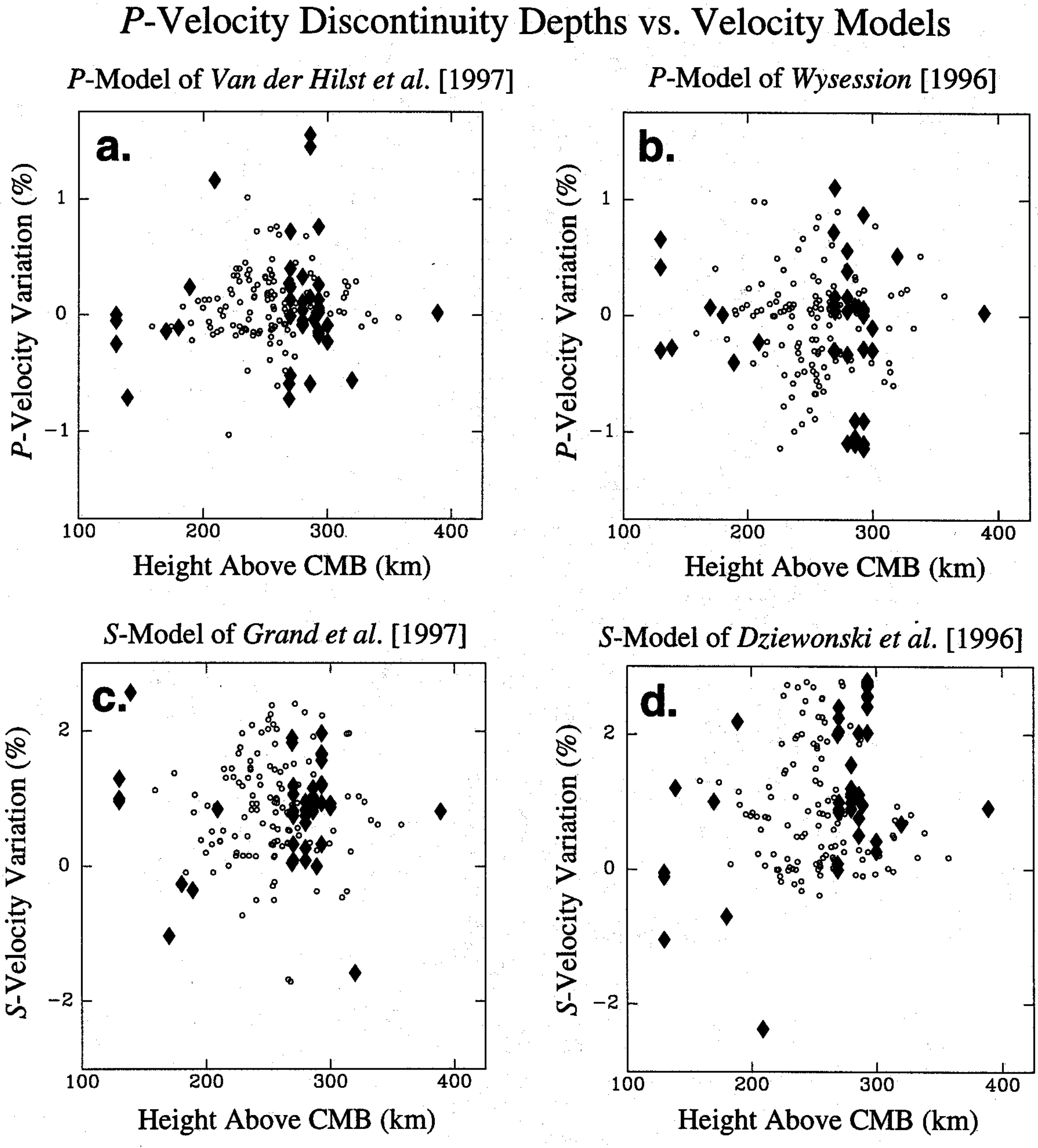

Figure 6. Plots showing the correlations between the variations in inferred D″ thickness, for both P and S velocities, and variations in the large-scale seismic velocities at the base of the mantle from four different seismic studies. In (a)-(d) the plots show V_P discontinuity thickness vs. the V_P velocity models of (a) *van der Hilst et al.* [1997], and (b) *Wysession* [1996a], and vs. the V_S velocity models of (c) *Grand et al.* [1997], and (d) *Dziewonski et al.* [1996]. In (e)-(h) the plots show V_S discontinuity thickness vs. the V_P velocity models of (e) *van der Hilst et al.* [1997], and (f) *Wysession* [1996a], and vs. the V_S velocity models of (g) *Grand et al.* [1997], and (h) *Dziewonski et al.* [1996]. Note that the correlations are poor. In (a)-(d), data shown is for *Weber and Körnig* [1992] (open circles) and P40 from Table 2 (solid diamonds). In (e)-(h), data shown is for *Lay et al.* [1997] (open circles), *Kendall and Shearer* [1994] and *Kendall and Nangini* [1996] (open triangles), and S16 from Table 2 (solid diamonds).

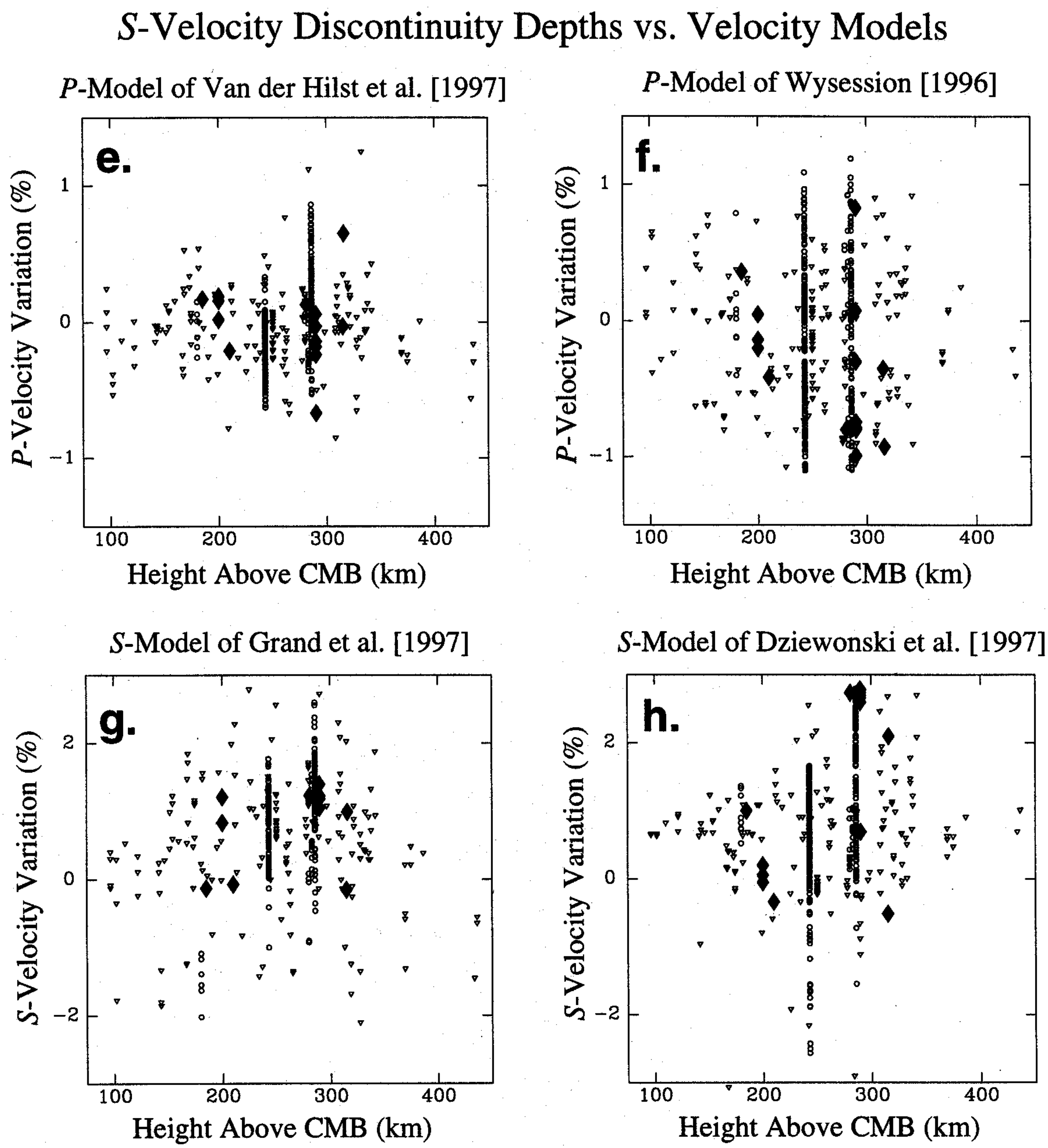

Figure 6. (continued)

temperature variations, as well as the locations of subducted slabs and hotspot origins [i.e., *Richards and Engebretson*, 1992; *Ricard et al.*, 1993]. Any correlation with the locations or topography of discontinuities could have important geodynamic and mineral physics implications. Table 2 and Figures 6*a-h* show these correlations, using a small sample of current velocity models of the lowermost mantle [*Grand et al.*, 1997; *Dziewonski et al.*, 1996; *van der Hilst et al.*, 1997; *Wysession*, 1996a]. While two models are of V_S [*Grand et al.*, 1997; *Dziewonski et al.*, 1996] and two are of V_P [*van der Hilst*, 1997; *Wysession*, 1996a], we show all possible correlations between these and the discontinuity parameters, with the strong caveat that correlations between P and S velocities at the base of the mantle may be poor [*Wysession et al.*, 1992; *Bolton and Masters*, 1996; *Robertson and Woodhouse*, 1996].

At first glance in Table 2 there seems to be an indication that D″ discontinuities might correlate with regions of fast velocity. For the locations of the 5 groups of observations (3 for V_S, and 2 for V_P), the *Grand et al.* [1997] model predicts increased mean V_S perturbations of 0.4 - 1.0%, and *Dziewonski et al.* [1996] predicts mean V_S values of 0.4 - 1.4%. However, *van der* Hilst [1997] predicts V_P perturbations of about 0%, and *Wysession* [1996a] predicts slightly negative V_P perturbations. It is more likely that these mean velocity values are the result of the limited geographical distributions of our discontinuity observations. Most relevant data sample D″ at very high latitudes, which tend to display faster V_S velocities than in V_P models [*Wysession*, 1996a].

There is also no significant difference between the average velocities of locations with and without discontinuities. The mean D″ velocities are the same in regions of discontinuities as in regions of non-observations (an average of +0.41% for both in the discontinuity-vs.-velocity model pairings in Table 2). The presence of a D″ discontinuity bears no indication of the presence of fast or slow average D″ velocities. One is just as likely to find a discontinuity or not in either fast or slow regions of D″.

There is also no significant correlation between the depths of D″ discontinuities and velocities at the base of the mantle from these 4 models. In Figures 6*a-d*, neither the V_P discontinuity depth data of P40 (diamonds) nor of *Weber and Körnig* [1992] (circles) correlate well with any of the velocity models. If Figures 6*e-h*, comparing V_S discontinuity depths with the velocity models, most of the correlations are small, with the exception of the S16 set, though this only has 16 values. However, correlations between the V_S discontinuity depths and the V_S models are all positive, suggesting a tendency for faster-than-average velocities at the base of the mantle in regions of elevated discontinuities. This would be expected if an increase in discontinuity elevation represented an increase in the total amount of fast D″ rock. No similar correlation is observed for the V_P discontinuities.

4.4. *Differences between P and S Discontinuities*

The D″ discontinuities for *P* and *S* waves exhibit similar characteristics. They are both found across wide geographical distributions, and observations are interspersed with non-observations over a range of spatial wavelengths (Plates 1 and 2). Both have similar mean depths, at about 240-260 km above the CMB. Direct comparisons are difficult because the different techniques required for working with *P* waves (e.g., stacking) and *S* waves (e.g., waveform modeling) result in few studies that examine both, though such studies find differences. *Weber* [1993] identified a region beneath NW Siberia with a similar discontinuity for both V_P and V_S, but also found a region beneath NW Siberia that had a discontinuity for V_S but not V_P, and two regions (Nansen Basin and Kara Sea) that had discontinuities for V_P but not V_S. *Ding and Helmberger* [1997] found a 3% discontinuity for V_S beneath Central America, but none for V_P.

One possibility is that the bulk and shear moduli change rapidly enough that D″ discontinuities for V_P and V_S actually appear and disappear over the small lateral scales observed in *Weber* [1993]. This would require lateral gradients comparable in strength to the radial gradients, effectively requiring blobs of chemically distinct material. Another possibility is that the different wavelengths for observed *PdP* and *SdS* phases are focussed differently by the discontinuity topography (or scale of volumetric heterogeneities). *Weber* [1993] estimates the Fresnel zones for 1 Hz *PdP* arrivals and lower frequency *SdS* arrivals to be 130 x 260 km and 230 x 460 km, respectively. If D″ topography is on the order of 100's of kilometers in scale, it could cause significant changes in the relative amplitudes of *PdP* and *SdS*, occasionally bringing one or both below noise levels.

An important test for this would come with the determination of a relevant comparison between the ratio of observations to non-observations for both V_P and V_S. There is an indication in Table 2 that there are many more V_S discontinuity observations than non-observations, and the opposite holds true for V_P. This observation is likely not to be significant because of the large differences between the studies. Not only are V_S and V_P data and analysis techniques different, but so are the degrees to which different studies have pursued non-observations, which are not as inherently interesting as discontinuity observations. Some data are also very close to each other and should perhaps count as single data. There are many reasons why such a comparison is not valid at this time. Nonetheless, an inference that the V_S discontinuity is in some way more robust or common than the V_P discontinuity would place an important constraint on the dominant wavelength of discontinuity topography or nature of a chemical discontinuity. If factors like the differences between V_S and V_P signal-to-noise thresholds can be assessed, differences in the ratio of observations to non-observations will be geophysically important.

There is likely to be a contribution to differences in the V_P and V_S discontinuities from actual differences between *P* and *S* velocities at the base of the mantle. *Grand et al.* [1997] find that while current mantle tomographic *P* and *S* velocity models agree very well throughout most of the mantle, this agreement significantly breaks down at the base of the mantle. This drop in correlation between *P* and *S* velocities in D″ was also observed by *Robertson and Woodhouse* [1996] and *Bolton and Masters* [1996]. *Wysession et al.* [1997], using *Pdiff* and *Sdiff* along identical paths, find the Poisson ratio drops from about 0.31 beneath the mid-Pacific to about 0.25 beneath Alaska. If D″ contains within it a chemical boundary layer [*Lay*, 1989], then it is likely that the chemical composition of this layer would vary laterally [*Davies and Gurnis*, 1986], resulting in lateral differences in the ratio between *P* and *S* velocities [*Wysession et al.*, 1992]. However, this will not be understood until more regions are examined with both *P* and *S* waves, and until we have a better sense of the effects of D″ discontinuity topography, which could distinguish between a chemical and thermal origin to D″ velocity anomalies.

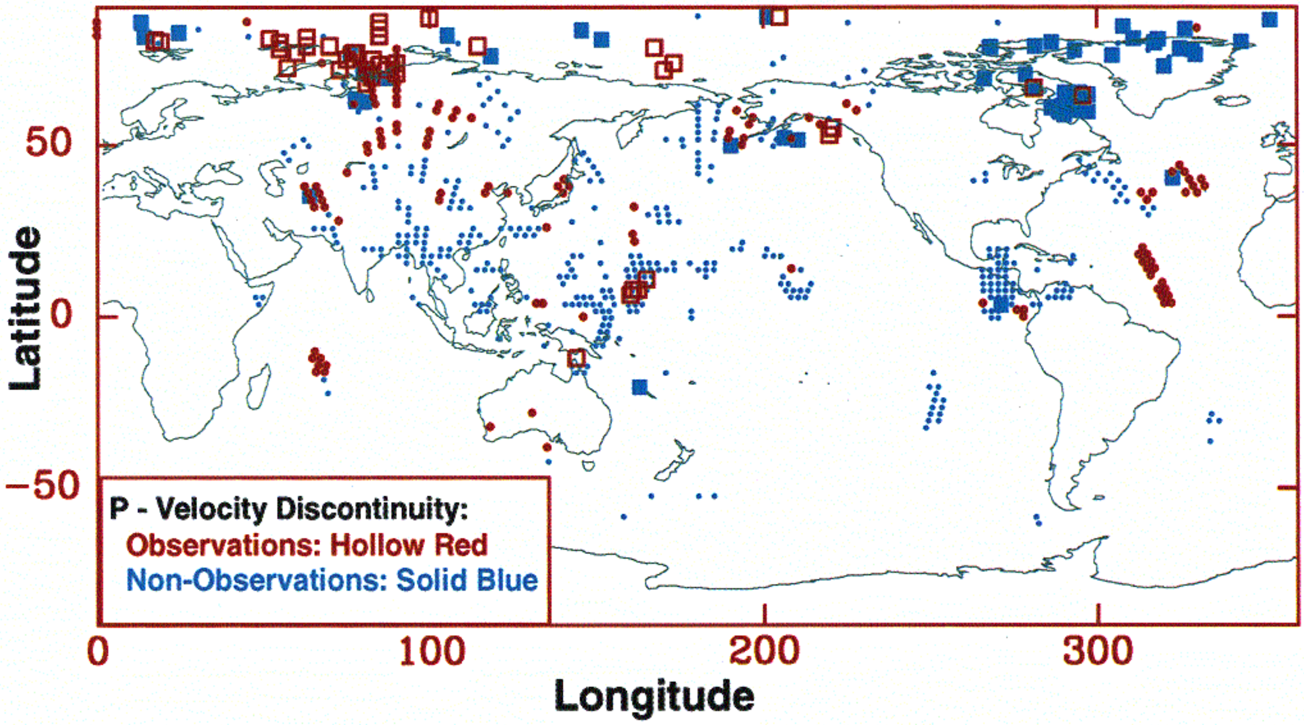

Plate 1. The geographical distributions of D″ V_P discontinuity observations and non-observations. Open red symbols are the locations of discontinuity observations, and closed blue symbols are non-observations. Circles are for ISC bulletin data from *Weber and Körnig* [1990, 1992]. Squares are a combination of studies, including *Weber and Davis* [1990], *Neuberg and Wahr* [1991], *Houard and Nataf* [1992, 1993], *Weber* [1993], *Vidale and Benz* [1993b], *Krüger et al.* [1993, 1995], *L. Breger and H.-C. Nataf* [personal communication], *Yamada and Nakanishi* [1996], *Ding and Helmberger* [1997], *Thomas and Weber* [1997], and *Sherbaum et al.* [1997], and represent composites of many waveforms.

4.5. Correlations with Levels of CMB Scattering

In searching for the origin of the *PdP* and *SdS* phases it is difficult to distinguish between a D″ discontinuity with topography and a distribution of 3D volumetric heterogeneities. With the former, the lower mantle-D″ impedance contrast is assumed to be constant, but topography causes focussing and defocussing that can turn the *PdP* or *SdS* phases on and off [e.g., *Schimmel and Paulssen*, 1996]. With the latter, horizontally varying impedance contrasts can turn *PdP* or *SdS* on and off, and scattering from heterogeneities within D″ can mimic the varying depths of discontinuity topography [*Sherbaum et al.*, 1997]. Conceptually the two models are very different, with a discontinuity appropriate for a sharp chemical or phase boundary, and 3D volumetric heterogeneities suggesting a process such as the accumulation of buckled oceanic crust or laminated CMB reaction products, or 3D phase transition variations due to localized thermochemical variations.

In some cases 1D models cannot adequately explain *PdP* and *SdS* observations. *Sherbaum et al.* [1997] show that *PdP* energy beneath the Arctic Sea does not always arrive along the earthquake-station great circle path, and suggest scatterers at a variety of depths. This was also found by *O'Mongáin and Neuberg* [1996] for *PdP* beneath Central America. However, CMB topography of the sort modeled by *Schimmel and Paulssen* [1996] could also provide *PdP* and *SdS* reflections detected at anomalous back-azimuths. *Sherbaum et al.* [1997] found that reflections from off-azimuth scatterers travel longer paths that look like deep 1D discontinuities, in some cases even from beneath the CMB, though *Lay and Young* [1996] migrated large data sets of *SdS* observations and found general compatibility with a horizontally extending discontinuity structure under Alaska. Further imaging efforts combined with synthetic 3D modeling [e.g., *Thomas and Weber* [1997] may reduce the wide range of distances above the CMB (100-440 km) assumed for 1D discontinuities.

Examining *Scd* phases beneath Alaska, Eurasia and India, *Lay et al.* [1997] found it difficult to distinguish between shear velocity heterogeneity of ± 4% within a 50 km thick region at the top of D″ and ± 50 km of discontinuity topography. In either case, a lack of correlation between *Scd* and *ScS* travel time residuals suggest that heterogeneity is

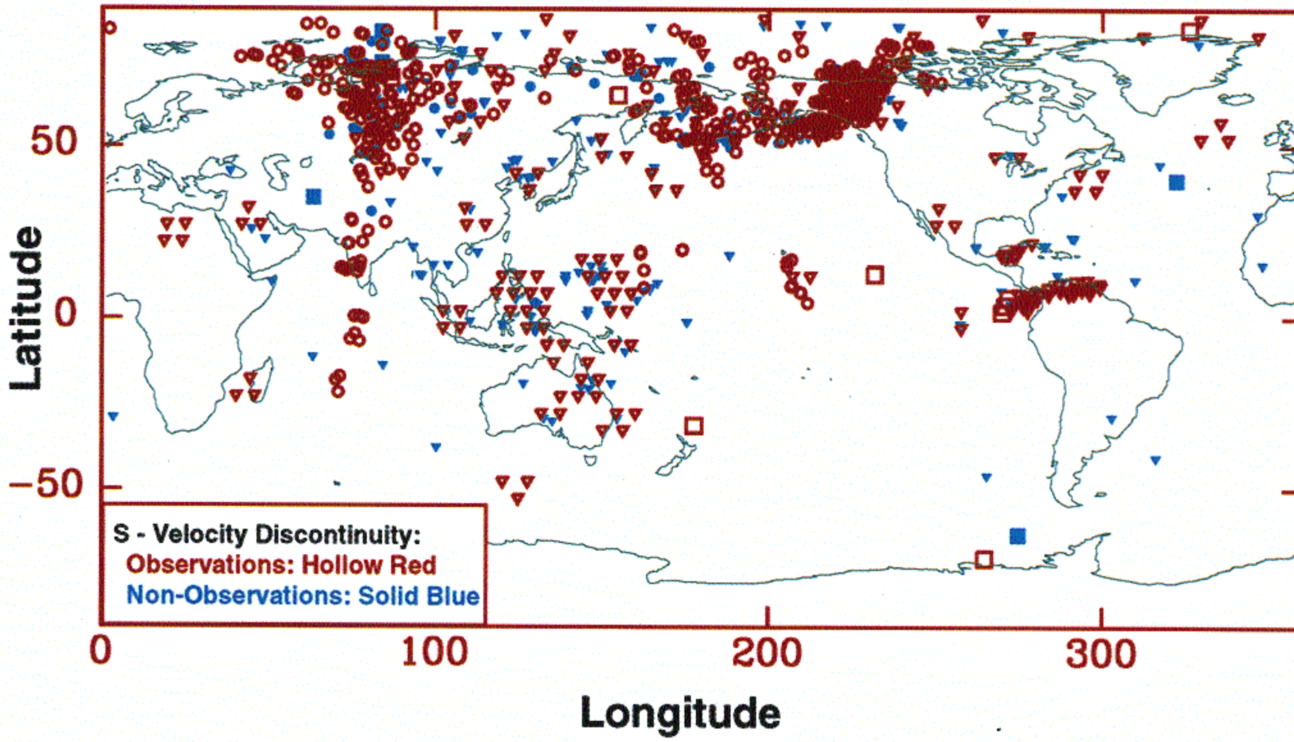

Plate 2. The geographical distributions of D″ V_S discontinuity observations and non-observations. Open red symbols are the locations of discontinuity observations, and closed blue symbols are non-observations. Triangles are for waveform data from *Kendall and Shearer* [1994] and *Kendall and Nangini* [1996]. Circles are for waveform data from *Lay and Helmberger* [1983], *Young and Lay* [1987b], *Young and Lay* [1990], *Gaherty and Lay* [1992], *Garnero et al.* [1993], and *Lay et al.*, [1997]. Squares are a combination of other studies, including *Weber and Davis* [1990], *Weber* [1993], *Schimmel and Paulssen* [1996], *Ding and Helmberger* [1997], *Valenzuela and Wysession* [1997], and *Olivieri et al.* [1997], and represent composites of many waveforms.

concentrated at the top of D″, and low levels of *ScS* fluctuation suggest that most of the rest of D″ is smoothly varying. If the ULVZ at the base of the mantle represents partial melting [*Williams and Garnero*, 1996], then reduced viscosities in the lower part of D″ may not be able to maintain the level of heterogeneity sustainable at the top. This model is consistent with model LAM+ of *Weber* [1994], originating from the accumulation of post-eclogite ocean crust brought down with paleoslabs. Additional support comes from the observations of *Lay et al.* [1997] that heterogeneity at the top of D″ seems to be decoupled from heterogeneities both within D″ and in the overlying mantle.

The scattering of seismic waves from the CMB region has been observed for a long time using *PcP* [*Vinnik and Dashkov*, 1970; *Frasier and Chowdhury*, 1974] and *PKP* [*Haddon and Cleary*, 1974; *Husebye et al.*, 1976], and more recently the codas of *Pdiff* [*Bataille et al.*, 1990; *Bataille and Lund*, 1996]. While these observations support lateral heterogeneity at scales as small as 10 km, they can be explained as either CMB topography of about 300 m or 3D volumetric heterogeneities of 1% distributed throughout a 200-km thick D″ [*Bataille et al.*, 1990]. Comparisons between regions of inferred D″ discontinuities and regions of increased *PKP* scattering is difficult due to incomplete geographical examinations of the latter. However, *Bataille and Flatté* [1988] looked at global *PKP* precursors and found no coherent model of regional scattering variations, concluding that the strength of these inhomogeneities is the same globally to within a factor of three. *Bataille and Flatté* [1988] could not distinguish between CMB topography and 3D volumetric heterogeneities within D″. It is possible that all *PKP* precursors do not have the same source. *Hedlin et al.* [1997] found that global heterogeneity is weak and distributed throughout the lower mantle, while *Vidale and Hedlin* [1998] found regional cases where strong *PKP* precursors may originate in a 60-km-thick layer at the base of D″.

5. IMPLICATIONS FOR MINERAL PHYSICS AND GEODYNAMICS

However numerous the speculations are about the CMB regions, there is only one reality, even if that reality involves a complicated set of regionally varying factors. Some combination of rock and/or liquid exists accounting for all of the unusual seismic observations. The presence of discontinuities, anisotropy, ultra-low velocity layers, and broad regional seismic velocity changes all have explanations, but because geological processes at 136 GPa and 3000-4000 K are likely to differ from those at STP conditions, these explanations remain uncertain. There are several possible factors that likely play major roles. There is either a discontinuity at the top of D″ or a distribution of heterogeneities within (though likely at the top of) D″. While the majority of the CMB is unsampled, the D″ discontinuity is likely globally extensive at a mean height of 250 km above the CMB, but with lateral variations of a strength comparable to the discontinuity itself. There is no correlation between the average lowermost mantle velocity and the occurrence of the discontinuity, and only a hint of one between average velocity and discontinuity thickness. There are no real differences between V_P and V_S. The D″ discontinuity seems to be superimposed upon regional D″ velocities, as it is found in hot (seismically slow) as well as cold (fast) regions, with some indications of systematic regional variations.

5.1. Discontinuity as an Isochemical Thermal Boundary

Because the CMB is much less dense than the underlying core, vertical heat transfer across the CMB in through conduction across D″, which thus contains (or is) a thermal boundary layer (TBL) with a large temperature gradient that remains poorly constrained [*Elsasser et al.*, 1979; *Stacey and Loper*, 1983; *Doornbos et al.*, 1986; *Boehler*, 1993]. An increase in temperature is compatible with the many recent seismic observations that support early suggestions of a decrease in velocities just above the CMB [*Kumagai et al.*, 1992; *Ritsema et al.*, 1997; *Valenzuela and Wysession*, 1997]. However, a simple TBL would not explain an *increase* in seismic-wave velocity. The CMB TBL likely plays only a moderate role in driving broad-scale mantle convection, as estimates of heat flux out of the core are typically 10-20% of that out of surface flux [*Davies*, 1988; *Sleep*, 1990]. This makes it difficult to explain large D″ variations with thermal effects alone, but it is possible for the remnants of slabs to accumulate at the CMB, causing a seismic velocity increase due to their cold signature superimposed upon TBL effects. The positive correlation between the height of the discontinuity above the CMB and corresponding tomographic-model D″ velocity for that location, though slight and not seen for all models, favors a thermal origin for the discontinuity over a chemical one. A chemical boundary layer would be pushed away and thinned in regions of downwelling, the opposite of what seems to be observed. It is also possible that the mechanisms creating the apparent D″ discontinuity differ in regions with and without recent subducted slab, and in paleoslab regions it is primarily of a thermal origin. Slabs may also provide a chemical signature (discussed later).

Could a strong decrease in temperature be the cause of the observed velocity increases atop D″? The major concerns are the magnitude of the required temperature increase and the steepness of the thermal gradient. Much experimental and theoretical work has been been pursued to estimate the seismic-wave velocities in D″, but as neither the exact composition nor prevalent phases of D″ are well established, this is a difficult problem. Guesses involving equations of state for likely lower mantle mineral assemblages have suggested that a 3% increase in seismic velocities would require a drop in temperature of about 700-1100°C [*Wysession et al.*, 1992]. Estimates by *Ding et al.* [1997] are at about 1100°C, and modeling by *Yuen et al.* [1994] (with data of *Chopelas* [1992], *Chopelas and Boehler* [1992], and *Chopelas et al.* [1993]) gives even higher estimates.

These numbers are large, but the cores of subducted slabs may be very cold compared to ambient temperatures at the base of the mantle. Three-dimensional numerical simulations predict that fossil slabs at the base of the mantle could have thermal anomalies exceeding 1000°C below the ambient lower mantle temperature [*Honda et al.*, 1993; *Steinbach et al.*, 1994], provided that the slab material reaches the base of the mantle in fast episodes of flushing [*Weinstein*, 1993; *Tackley et al.*, 1993]. *Ding et al.* [1997] suggest 700°C as the temperature decrease of ponded fossil slab at the CMB relative to the lower mantle adiabat. The rate of descent of slabs through the highly-viscous lower mantle is a key factor in the prediction of lower mantle slab temperatures. Seismic tomography shows a broadening of the slab signature across the 660 km discontinuity in some regions [*Grand et al.*, 1997], and this thickening or buckling suggests a decrease in slab velocities, perhaps a result of increased viscosity in the lower mantle. Slower descent of slabs means greater thermal assimilation of the outer part of the slab by the time it reaches the CMB, but a greater distance for heat to conduct from the core of the slab. The effect would be a broader boundary zone across which a large ΔT might be maintained.

The thickness of this boundary transition is important because of the constraints placed by seismic observations. *S*-velocity studies suggest a maximum thickness of 50 km [*Revenaugh and Jordan*, 1991*a,b*] to 75 km [*Young and Lay*, 1987b; *Weber et al.*, 1996], but *P*-velocity studies may demand the transition to be less than 8 km [*L. Breger and H.-C. Nataf*, personal communication]. It is hard to envision a ΔT of 700-1100°C across less than 8 km at the top of D″, a distance having a thermal diffusion time of less than 5 million years. Distributed across a 50-75 km distance, such a thermal boundary would be more plausible. Certain geodynamic mechanisms might aid in this. If cold slab rock ponded laterally across the CMB, it could displace lower-viscosity hot rock from the base of D″ up and over the ponded slab [*Stevenson*, 1993], enhancing the thermal transition. Seismic observations may support this, modeling velocities above the D″ discontinuity as slower than expected for several hundreds of km into the mantle.

Ding et al. [1997] use numerical modeling to predict that the thermal anomalies resulting from the subduction of the Farallon slab can adequately explain both the existence of the D″ discontinuity as well as large-scale tomographic seismic images. The temperature through a vertical profile across their modeled slab at the CMB shows a decrease in temperature of around 700°C at the coldest point (a depth of about 2700, the location of the D″ discontinuity) from ambient lower mantle temperatures, and then an increase at the base of D″ to about 3300°K. *Ding et al.* [1997] use the approach of *Zhao and Anderson* [1994] to interpret the temperature decrease as a shear velocity increase of 2.5%, distributed over a vertical range of a few hundred kilometers. Even though the seismic modeling still invokes a first-order discontinuity at the top of D″, not found in the geodynamic model, the *Scd* data is best fit by a seismic model where most of the velocity increase occurs gradually over a vertical range of 120 km. *Ding et al.* [1997] suggest a thermal origin to the D″ discontinuity, as the *SdS* triplication has traditionally been best found beneath regions of convective downwellings [*Lay*, 1995], and that a chemical boundary layer would be dispersed by such downwellings.

A concern with a purely thermal explanation for the D″ discontinuity is its lateral extent, as it has been observed in regions with no recent subduction and in regions presumed to be anomalously hot. Is it possible for cold slab to entirely cover the CMB and retain a strong enough thermal signature to provide the discontinuity? Lithosphere is subducting at the current rate of about 3 km^2/yr (or 240 km^3/yr assuming an 80 km thick oceanic lithosphere) so the circulation time required to fill up and empty a 250 km thick D″ layer, assuming complete full-mantle circulation, would be about 170 Ma. Since the rock slab is likely to take at least this long to reach the CMB from the surface (not counting mantle avalanche processes), we would require the cold thermal anomaly to last in the mantle for over 350 Ma, unrealistic because the characteristic distance for thermal diffusion is 100 km for such time-scales, and thermal equilibration is hastened by flux of core heat across larger thermal gradients.

Due to the effects of thermal equilibration, the amount of material which is sufficiently cold to generate a 3% velocity contrast is likely to be a relatively small volumetric portion of the slab at CMB depths, and even this portion will be intercalated with warmer (and thus less seismically anomalous) material. Therefore, to produce a relatively broadly distributed laminar boundary with a typical height above the CMB of 250 km through purely thermal effects requires a number of rather specific geodynamic phenomena to occur above the CMB: 1) preservation of sufficient cold slab material to produce the notable seismic velocity contrasts, including possible segregation of cold slab material from surrounding thermally equilibrated material; 2) emplacement of the cold slab material at a height near 250 km above the CMB; and 3) broadly horizontal emplacement of the cold material. Perhaps the most difficult of these conditions to satisfy from a thermal perspective is the predominance of discontinuity depths in the 200-300 km range (Figure 5). It is unclear why colder (and hence denser) material should be emplaced at this height above the CMB rather than at a range of depths down to the mantle's base, particularly if segregation of cold material from warm material can readily occur at these depths. Although the regional temperature fields of slabs descending to the core-mantle boundary would be anticipated to generate local velocity heterogeneities, there are difficulties with the 250 km discontinuity produced only thermally, unless very rapid mantle avalanches bring large amounts of slab material to the CMB.

It may also be possible that the seismological results are pointing toward a thicker TBL at the base of the mantle. The seminal study of *Stacey and Loper* [1983] used the seismic model PREM [*Dziewonski and Anderson*, 1981] to derive a quasi-exponential thermal profile with a scale height of 73 km and a maximum thermal gradient of 11.2 K/km. The PREM model represented D″ as a 150 km layer in which the bulk modulus pressure derivative was unusually low (1.64 instead of about 3.2 in the overlying mantle), and the vertical shear velocity gradient was very slightly negative. Recent work suggests a more dramatic TBL with very strong negative shear velocity gradients extending over the bottom 200-250 km of the mantle. This seems to hold true both beneath discontinuities in fast areas [*Young and Lay*, 1990; *Gaherty and Lay*, 1992] and in the slow velocities of the Pacific [*Ritsema et al.*, 1997; *Valenzuela and Wysession*, 1997], suggesting that the D″ thermal boundary layer is much larger than 75 km. Such a thick TBL would require higher viscosities or densities at the base of the mantle to suppress instabilities that could break up the TBL.

5.2. *Discontinuity as an Isochemical Phase Boundary*

Mineralogical phase changes play an important role in upper mantle geodynamics, and it is possible that the same holds for the lower mantle [*Bina*, 1991]. Even though the lower mantle is viewed as being largely homogeneous and adiabatic, there have been identifications of seismic discontinuities at depths of 710, 900, and 1200 km [*Revenaugh and Jordan*, 1991b; *Wicks and Richards*, 1993], and this may also be the case for D″. A 3% D″ velocity increase is significant compared to upper mantle discontinuities (the 660 km discontinuity is 4.7% for *P* and 7.0% for *S*), as the high pressures at the CMB cause minerals to be much more incompressible, and might only occur from a breakdown of a major lower mantle phase like perovskite. *Stixrude and Bukowinski* [1992] demonstrated that the breakdown of $(Mg,Fe)SiO_3$ perovskite to its constituent oxides is unlikely to explain the D″ discontinuity, but other transformations, perhaps involving Ca and Al, may contribute.

The multi-component phase equilibria of the mantle under CMB conditions remains uncertain, although the approximate mineralogic end-members assumed to predominate under deep mantle conditions have each been examined to pressures approaching those of the CMB. In particular, (Mg,Fe)SiO_3-perovskite, $CaSiO_3$-perovskite and (Mg,Fe)O have been probed statically to pressures of 112, 134 and 95 GPa, with (Mg,Fe)O having been examined under shock to pressures exceeding those of the CMB [*Knittle and Jeanloz*, 1987; *Mao et al.*, 1989; *Mao and Bell*, 1979; *Vassiliou and Ahrens*, 1982]. None of these end-members undergoes a resolvable phase transition at pressures corresponding to the lowermost mantle, but there are indications that the partitioning behavior of iron between perovskite and magnesiowüstite could shift depending on the valence state of iron and the aluminum content of deep mantle materials [*Wood and Rubie*, 1996; *McCammon*, 1997]. Aluminum produces enhancements in the amount of iron (particularly as Fe^{3+}) entering into the perovskite structure relative to that which would be inferred from results in the MgO-FeO-SiO_2 system [*Ito et al.*, 1994; *Fei et al.*, 1991; *Kesson and Fitz Gerald*, 1991]. Whether enhanced iron contents in deep mantle perovskite could generate exsolution of Fe or Al-rich phases (possibly with free silica) remains unclear.

All the upper mantle phase transitions, driven by pressure increases, involve increases in seismic velocities. Densities increase, but are over-compensated by increases in incompressibility and rigidity. The same would have to hold for a D″ phase transition. Lateral variations in composition as well as temperature might create topography on such a phase change, the way the 660 km discontinuity is depressed by the cold temperatures of subducting slabs [*Shearer and Masters*, 1992]. However, the seismic observations suggest changes in topography of several hundred kilometers. This would require a very steep Clapyron slope for the phase transition, with very small changes in temperature resulting in very large changes in the pressure at which the transition occurs. If perovskite, the most abundant mineral structure within the Earth, were to break down into an assemblage containing phases like (Mg,Fe)O, SiO_2 and Al_2O_3, would this cause a 3% increase in seismic velocities? The high seismic velocities of SiO_2 stishovite [*Sherman*, 1993] might be able to over-compensate for the slower seismic velocities of (Mg,Fe)O to provide an overall increase in seismic velocity [*Wysession*, 1996b]. The transformation would also have to explain why the D″ discontinuity is roughly the same (about 3%) for both V_P and V_S, as lateral *S*-velocity variations at the base of the mantle are greater than for *P*-velocities ($\delta \ln V_S / \delta \ln V_P \cong 4$ [*Grand et al.*, 1997; *Wysession and Kuo*, in preparation]). The largest concern with a phase change as the cause of D″ is that it has yet to be experimentally observed, and so remains speculative.

5.3. Discontinuity as a Thermo-Chemical Boundary

Whether or not the thermal signature of slabs or a mineralogical phase change is responsible for the D″ discontinuity, it is probable that chemical heterogeneities play a significant part. The high temperature contrast across the core-mantle boundary required by the high temperatures in the outer core [*Williams et al.*, 1991] should lead to vigorous development of upwellings from the thermal boundary layer, yet the contribution of the core-mantle boundary to the surface heat budget is relatively minor. This suggests that a stable chemical boundary layer (CBL) is present, reducing heat flow across the associated TBL and makes instabilities across the CMB less important to the Earth's surface heat flow. *Bullen* [1949] postulated a chemically inhomogeneous boundary layer as the cause for the seismic D″, and numerous studies have discussed the implications for chemical heterogeneity or a CBL at the base of the mantle [i.e., *Davies and Gurnis*, 1986; *Gurnis*, 1986; *Gurnis and Davies*, 1986; *Ahrens and Hager*, 1987; *Schubert et al.*, 1987; *Zhang and Yuen*, 1987, 1988; *Hansen and Yuen*, 1988, 1989; *Silver et al.*, 1988; *Sleep*, 1988; *Stevenson*, 1988; *Christensen*, 1989; *Knittle and Jeanloz*, 1989, 1991; *Lay*, 1989; *Buffett et al.*, 1990; *Olson and Kincaid*, 1991; *Revenaugh and Jordan*, 1991b; *Ringwood and Hibberson*, 1991; *Stacey*, 1991; *Goarant et al.*, 1992; *Wysession et al.*, 1992, 1993; *Boehler*, 1993; *Buffett*, 1993; *Jeanloz*, 1993; *Kellogg and King*, 1993; *Poirier*, 1993; *Yuen et al.*, 1993, 1994; *Christensen and Hofmann*, 1994, *Weber*, 1994; *Loper and Lay*, 1995; *Kendall and Silver*, 1996; *Lay et al.*, 1997, 1998; and others].

There is a difficulty, however, in finding a mineral assemblage that is both dense enough to be stable at the base of the mantle and seismically fast enough to provide the observed 2-3% increase over ambient lower mantle velocities. For example, increasing density by increasing the iron content of the assemblage, either by a decreased silicate magnesium number or by added iron alloys, will likely reduce seismic velocities. Purely compositional explanations for the possible genesis of layering in D″ can be loosely divided into four categories: 1) descent and segregation of subduction-related geochemical heterogeneities into D″, in the form of subducted basaltic crust and its complementary harzburgite [*Christensen and Hofmann*, 1994]; 2) interaction of the lowermost mantle with the outer core, producing iron enrichment of the lowermost mantle through chemical reactions with outer core material [*Knittle and Jeanloz*, 1989; *Goarant et al.*, 1992];3) preservation of primordial stratification of the planet either through enrichment of refractory oxides in a modified heterogeneous accretion scenario [*Ruff and Anderson*, 1980] or through the preservation of fossilized remnants of magma ocean solidification; or 4) descent of dense, possibly molten material into D″ over time, which could produce progressive geochemical enrichment of this region in incompatible elements [*Rigden et al.*, 1988]. Of these explanations, any primordial stratification which persisted over the age of the planet would only be preserved if it were denser than the overlying mantle: such a density difference is not consistent with the intermittent presence of this discontinuity in a hot, inviscid thermal boundary layer. Core-mantle reactions present a more complex set of possibilities. Iron enrichment typically produces a decrease in seismic velocities, and the products of core-mantle reactions likely follow this trend [e.g., *Williams and Garnero*, 1996]. However, these reactions produce both iron-free $MgSiO_3$-perovskite and SiO_2 as reaction products (which are anticipated to be comparatively high velocity constituents), in addition to FeO and FeSi. If the core and mantle have reacted extensively over time, and pervasive segregation of iron-free from iron-rich reaction products can occur, then a possible (although somewhat restrictive) mechanism exists for producing an enrichment of D″ in relatively high velocity components.

Considerable attention has been focussed on shifts in silica content with depth in the mantle in the past [e.g., *Stixrude et al.*, 1992], partially motivated by the differences in chemistry between peridotitic and chondritic compositions. Silica enrichment also has the tendency to increase seismic velocity, providing possible chemical explanations for the 250-km D″ discontinuity. The observation that basaltic material contains free SiO_2 at deep mantle pressures is significant [*Kesson et al.*, 1994], and provides an additional means by which silica could be enriched in D″. It has been proposed that small degrees of partial melting may be present in portions of the lower mantle characterized by high values of $d\ln V_S/d\ln V_P$ [*Duffy and Ahrens*, 1992]. While the melting behavior of the deep mantle remains uncertain, any descent of deep mantle melts into D″ could alter the chemistry of this region relative to the overlying mantle, so the existence of moderate SiO_2 enrichment of the lowermost mantle cannot be precluded. Whether SiO_2 enrichment can generate the 250 km discontinuity hinges on its elastic and phase properties under CMB conditions [*Tsuchida and Yagi*, 1989; *Dubrovinsky et al.*, 1997].

Accepting whole mantle convection, there is a possibility of a delamination and accumulation of post-eclogitic ocean crust at the base of the mantle [*Gurnis*, 1986; *Gurnis and Davies*, 1986; *Silver et al.*, 1988; *Christensen*, 1989; *Olson and Kincaid*, 1991]. *Gurnis and Davies* [1986] demonstrated that the recycling of oceanic crust could play an important role in generating the observed geochemical heterogeneity of the mantle. However, unless the crustal component is at least neutrally buoyant compared to the rest of the subducting slab, it may be difficult to separate the crustal component from the rest on the time scale required for transport of a subducting slab to the lowermost mantle [*Richards and Davies*, 1989]. *Christensen and Hofmann* [1994] used numerical simulations to model the delamination of basaltic crust from subducting slabs, the ponding of the former basalt at the base of the mantle, and the re-entrainment of the material in hotspot plumes, providing an explanation for why more enriched isotope ratios are linked to mantle plumes. They estimated that the density of the subducted crust was large enough (by 1.5-2.3%) to accumulate in D″, but not too large to be entrained in the upflow of mantle plumes. *Christensen and Hofmann* [1994] predict that MORB anticrust at the CMB could be up to 25 wt% SiO_2 stishovite, and the resulting anticrust compositions could provide the observed 2-3% seismic velocity increase [*Wysession*, 1996b]. The stabilization of Ca- (+/- Al-) bearing silicate perovskite in basaltic compositions may also lead to enhanced velocities [*Funamori and Jeanloz*, unpublished work]. Because of the return of anticrust to the surface (on the basis of OIB isotope ratios), *Christensen and Hofmann* [1994] suggest that anticrust occupies only 3-15% of D″ at any given time, but *Weber* [1994] showed that a thin layer of anomalously fast laminates (model LAM+) at the top of D″ could explain many properties of the *PdP* observations. This is also in keeping with results of *Lay et al.* [1997] that *Scd* anomalies, more pronounced than for *ScS*, accumulated near the top of D″ and were compatible with ±4% V_S variations within a 50 km thick region (and/or ± 50 km of discontinuity topography). *Lay et al.* [1997] found the uppermost portion of D″ to be more heterogeneous than the deeper parts of D″.

The other common candidate for the origin of D″ heterogeneity is the by-product of core-mantle chemical reactions, as observed in laser-heated diamond anvil cells [*Knittle and Jeanloz*, 1989, 1991; *Goarant et al.*, 1992; *Jeanloz*, 1993], where $(Mg,Fe)SiO_3$ perovskite reacts with liquid iron to form $MgSiO_3$, SiO_2, and FeO and FeSi metallic alloys. The metallic alloys will not provide any fast velocities, but they will also be dense enough to resist being brought to the top of D″. If the SiO_2 stishovite were swept to the top of D″ it would be a likely candidate for the D″ discontinuity. Further experimentation must be done, as there is an indication that dry CMB conditions would favor reactions between iron and MgO rather than iron and perovskite [*Boehler*, 1993].

Because we have a poor understanding of the TBL and viscosity structure of D″, it is impossible to predict exactly how heterogeneities would be transported within D″, though many studies have given an indication of the possible modes of transport [*Davies and Gurnis*, 1986; *Gurnis*, 1986; *Gurnis and Davies*, 1986; *Schubert et al.*, 1987; *Zhang and Yuen*, 1987, 1988; *Hansen and Yuen*, 1988, 1989; *Sleep*, 1988; *Stevenson*, 1988; *Christensen*, 1989; *Olson and Kincaid*, 1991; *Kellogg and King*, 1993; *Christensen and Hofmann*, 1994]. The dynamics will be controlled largely by the density contrast created by any existent heterogeneity. Most numerical and laboratory models indicate that a density contrast ≥ 3-6% is required to maintain a stable layer; at lower densities, heterogeneities are gradually entrained in mantle plumes, so the CBL must be resupplied if it is to persist for long. Thus the residence time for heterogeneities in a CBL depends critically on the density contrast, which is yet unknown.

The structure of a CBL also depends on how buoyant it is. A very stable CBL is largely isolated from lower mantle circulation and will likely exhibit little topography or lateral variability. Whether the CBL is made up of subducted oceanic crust, CMB reaction products, or both, it is more likely to be marginally stable (with a $\Delta\rho \approx 2\%$). Numerical simulations indicate that a marginally stable layer tends to pile up under upwellings and thin beneath downwellings [e.g *Hansen and Yuen*, 1988, 1989]. Internal circulation within the

CBL complicates the structure so that upwellings do not necessarily correlate with the thickest CBL regions [e.g. *Hansen and Yuen*, 1989; *Kellogg and King*, 1993].

If motions are dominated by large-scale flow driven by the ponding of slabs and/or the generation of large mantle plumes, laminar heterogeneities would be stretched horizontally in most places except the base of plumes where they may take a more vertical orientation. Such structures have been proposed to explain the unusual nature of D″ anisotropy, with transverse isotropy dominating in D″ regions of mantle slab downwellings but azimuthal anisotropy observed in D″ beneath the mid-Pacific plume groups [*Lay et al.*, 1998]. We would expect a well-defined CBL to be moved about laterally by the mantle flow, thinned in regions of downwelling and thickened beneath upwellings. As no obvious correlation is observed between the height of the D″ discontinuity and regions of downwellings and upwellings (as represented by large-scale velocity models), if such a stable CBL exists, this is likely not what *PdP* and *SdS* waves are detecting. Internal circulation can be driven by the overlying flow (upwelling plumes and downwellings) or by convection within the CBL itself. The CBL is not likely to convect internally if its thermal structure is determined primarily by the presence of cold slabs. On the other hand, if the viscosity in D″ is low enough, there could be internal convection within D″ that would create local pockets of variable composition within the D″ layer but isolate the layer from the overlying mantle. Internal convection creates a secondary thermal boundary layer at the top of the CBL as well as a TBL at the core-mantle boundary. The resulting TBL's above and below a layer with a quasi-adiabatic interior are not, however, in agreement with seismic observations that favor a strong negative gradient throughout D″.

The upshot is that chemical heterogeneities are likely to exist in D″, whether they are a primitive differentiated layer, core-mantle reaction products, delaminated oceanic crust, or the result of ongoing mid-mantle differentiation, and are likely to be related to the anomalous seismic observations seen in the form of seismic anisotropy and the D″ discontinuity. Just as continental crust influences convection patterns of the upper mantle, a CBL at the CMB will influence flow in the overlying mantle. Plumes rising from the top of a combined CBL and TBL tend to be hotter [*Farnetani*, 1997] and more stable in position [*Kellogg*, 1997] than plumes rising from an isochemical TBL.

6. CONCLUSIONS

The D″ discontinuity remains one of the most enigmatic seismic features of the Earth. Since the postulation [*Wright*, 1973; *Wright and Lyons*, 1975, 1981] and discovery [*Lay and Helmberger*, 1983] of the feature, over 40 publications have presented observations and interpretations of seismic waves interacting with the D″ discontinuity. And yet there is still no consensus as to what form the discontinuity takes and what is causing it. The height of the discontinuity is seen to range from 100-450 km above the CMB, though the mean height for both *P* and *S* velocities is about 250-265 km above the CMB. A vertical discontinuity transition width of 50-75 km is compatible with most data, though some work with high frequency waves suggests it might be thinner in some places. The velocity increase is generally about 2-3% above that of the overlying mantle (again, the same for both *P* and *S* velocities), when the discontinuity is observed. The geographical distribution of the D″ discontinuity is such that it is both observed and not observed in most places of the CMB where it has been pursued. The discontinuity can sometimes turn on and off over very short distances (10-100 km), and other times behave coherently over much larger distances (> 1000 km). While many of the observations occur beneath Alaska and the Caribbean, which are the likely repositories of Mesozoic subducted slabs [*Ricard et al.*, 1993; *Grand et al.*, 1997], there is no difference between the average D″ velocity (from tomographic models) for locations of discontinuity observations and locations of non-observations. However, there is a slight positive correlation between the height of the inferred D″ discontinuity above the CMB and the regional velocity in the vicinity of the discontinuity as determined from tomographic models. This might suggest a preference toward a thermal rather than chemical origin for the discontinuity.

The source of the D″ discontinuity could be either a true surface, with large amounts of topography to explain both the range in depths observed as well as the the ability for the discontinuity to turn on and and off through focusing and defocussing effects, or a distribution of heterogeneities distributed within D″. Such a surface could be (1) thermal, representing the top of ponded subducted slab material, (2) mineralogical, representing a phase boundary between two different sets of phase assemblages, or (3) chemical, representing the separation between two different heterochemical regions. The alternate model, of scattered heterogeneities, could represent chemical or phase anomalies (triggered by slight chemical anomalies) distributed by convective patterns at the base of the mantle. These chemical anomalies may come from core-mantle reactions, the delamination of oceanic crust, or whole-mantle differentiation (either primordial or concurrent). It is likely that thermal, phase and chemical anomalies are all present, and even possible that the D″ discontinuity could have different causes in different locations. It is also likely that the D″ discontinuity is intimately related to the process of seismic anisotropy within D″. More work is needed to determine the geographical extent of the discontinuity, to model the seismic observations in three-dimensions, to determine the thermal structure of D″, to identify the phase relations of minor as well as major minerals at CMB conditions, and understand the possible mechanisms of convective mixing under these conditions.

Acknowledgments. This research was supported by NSF grants EAR-9305894 (TL), EAR-9418643 (TL), EAR-93-05892 (LK), EAR-9417542 (MW), and the Packard Foundation (MW). CMB workshops organized under EAR-9305894 helped develop interdisciplinary coordination on this topic. Contribution 338 of the Institute of Tectonics and W. M. Keck Seismological Laboratory.

REFERENCES

Ahrens, T. J., and B. H. Hager, Heat transport across D" (abstract), *Eos Trans. AGU, 68*, 1493, 1987.

Bataille, K., and S. M. Flatté, Inhomogeneities near the core-mantle boundary inferred from short-period scattered *PKP* waves recorded at the Global Digital Seismograph Network, *J. Geophys. Res., 93*, 15,057-15,064, 1988.

Bataille, K., and F. Lund, Strong scattering of short-period seismic waves by the core-mantle boundary and the *P*-diffracted wave, *Geophys. Res. Lett.*, 23, 2413-2416, 1996.

Bataille, K., R. S. Wu, and S. M. Flatté, Inhomogeneities near the core-mantle boundary evidenced from scattered waves: A review, *Pure Appl. Geophys., 132*, 151-174, 1990.

Baumgardt, D. R., Evidence for a *P*-wave velocity anomaly in D", *Geophys. Res. Lett., 16*, 657-660, 1989.

Bina, C. R., Mantle Discontinuities, *Rev. Geophys., U.S. National Rep. to International Union of Geodesy and Geophysics 1987-1990*, 783-793, 1991.

Boehler, R., Core-mantle reactions? (abstract), *Eos Trans. AGU, 74*(43), Fall Meeting Supp., 415, 1993.

Bolton, H., and G. Masters, A region of anomalous *dlnVs/dlnVp* in the deep mantle (abstract), *Eos Trans. AGU, 77*(46), Fall Meeting Supp., F697, 1996.

Buffett, B. A., Influence of a toroidal magnetic field on the nutations of Earth, *J. Geophys. Res., 98*, 2105-2117, 1993.

Buffett, B. A., T. A. Herring, P. M. Matthews, and I. I. Shapiro, Anomalous dissipation in Earth's forced nutations: Inferences on the electrical conductivity and magnetic energy at the core-mantle boundary (abstract), *Eos Trans. AGU, 71*, 496, 1990.

Bullen, K. E., Compressibility-pressure hypothesis and the Earth's interior, *Month. Not. R. Astr. Soc., Geophys. Suppl., 5*, 355-368, 1949.

Chopelas, A., Sound velocities of MgO to very high compression, *Earth Planet. Sci. Lett., 114*, 185-192, 1992.

Chopelas, A., and R. Boehler, Thermal expansivity in the lower mantle, *Geophys. Res. Lett.*, 19, 1983-1986, 1992.

Chopelas, A., H. J. Reichmann, and L. Zhang, Sound velocities of four minerals to very high compression: constraints on $\delta \ln\rho/\delta \ln V$ in the lower mantle, *EOS, Trans. Am. Geophys. Un., 74* (16), 41, 1993.

Christensen, U. R., Models of mantle convection: one or several layers, *Philos. Trans. R. Soc. London A, 328*, 417-424, 1989.

Christensen, U. R., and A. W. Hofmann, Segregation of subducted oceanic crust in the convecting mantle, *J. Geophys. Res., 99*, 19,867-19,884, 1994.

Cleary, J. R., The D" region, *Phys. Earth Planet. Inter., 30*, 13-27, 1974.

Creager, K. C., and T. H. Jordan, Aspherical structure of the core-mantle boundary from *PKP* travel times, *Geophys. Res. Lett., 13*, 1497-1500, 1986.

Dahm, C. G., New values for dilatational wave-velocities through the Earth, *Trans., Am. Geophys. Union*, 80-83, 1934.

Davies, G. F., Ocean bathymetry and mantle convection, 1, Large-scale flow and hotspots, *J. Geophys. Res., 93*, 10,447-10,480, 1988.

Davies, G. F., and M. Gurnis, Interaction of mantle dregs with convection: lateral heterogeneity at the core-mantle boundary, *Geophys. Res. Lett., 13*, 1517-1520, 1986.

Ding, X., and D. V. Helmberger, Modeling D" structure beneath Central America with broadband seismic data, *Phys. Earth Planet. Inter., 101*, 245-270, 1997.

Ding, X., Sidorin, I., Helmberger, D. V., Gurnis, M., and Grand, S., D" seismic structure in down-welling regions, *Geophys. Res. Lett.*, submitted, 1997.

Doornbos, D. J., S. Spiliopoulos, and F. D. Stacey, Seismological properties of D" and the structure of a thermal boundary layer, *Phys. Earth Planet. Int., 41*, 225-239, 1986.

Dubrovinsky, L. S., S. K. Saxena, P. Lazor, R. Ahuja, O. Eriksson, J. M. Wills, and B. Johansson, Experimental and theoretical identification of a new high-pressure phase of silica, *Nature, 388*, 362-365, 1997.

Duffy, T. S., and T. J. Ahrens, Sound velocities at high pressure and temperature and their geophysical implications, *J. Geophys. Res.*, 97, 4503-4520, 1992.

Dziewonski, A. M., and D. L. Anderson, Preliminary reference earth model, *Phys. Earth Planet. Inter., 25*, 297-356, 1981.

Dziewonski, A. M., G. Ekström, and X.-F. Liu, Structure at the top and bottom of the mantle, in *Monitoring a Comprehensive Test Ban Treaty*, Kluwer Academic Publishers, pp. 521-550, 1996.

Elsasser, W. M., P. Olson, and B. D. Marsh, The depth of mantle convection, *J. Geophys. Res., 84*, 147-155, 1979.

Farnetani, C. G., Excess temperature of mantle plumes: The role of chemical stratification across D", *Geophys. Res. Lett, 24*, 1583-1586, 1997.

Fei, Y., H.-K. Mao, and B. O. Mysen, Experimental determination of element partitioning and calculation of phase relations in the MgO-FeO-SiO_2 system at high pressure a high temperature, *J. Geophys. Res., 96*, 2157-2170, 1991.

Frasier, C., and D. K. Chowdhury, Effect of scattering of *PcP/P* amplitude ratios at LASA from 40° to 84° distance, *J. Geophys. Res., 79*, 5469-5477, 1974.

Gaherty, J. B., and T. Lay, Investigation of laterally heterogeneous shear velocity structure in D" beneath Eurasia, *J. Geophys. Res., 97*, 417-435, 1992.

Garnero, E. J., and T. Lay, Lateral variations in lowermost mantle shear wave anisotropy beneath the north Pacific and Alaska, *J. Geophys. Res., 102*, 8121-8135, 1997.

Garnero, E. J., D. V. Helmberger, and G. Engen, Lateral variations near the core-mantle boundary, *Geophys. Res. Lett., 15*, 609-612, 1988.

Garnero, E. J., D. V. Helmberger, and S. Grand, Preliminary evidence for a lower mantle shear wave velocity discontinuity beneath the central Pacific, *Phys. Earth Planet. Int., 79*, 335-347, 1993.

Garnero, E. J., J. Revenaugh, Q. Williams, T. Lay, and L. Kellogg, Ultra-low velocity zone at the core-mantle boundary, in *Observational and Theoretical Constraints on he Core-Mantle Boundary Region*, ed. by M. Gurnis, M. Wysession, B. Buffett and E. Knittle, AGU, Washington, D. C., this volume, 1998.

Goarant, F. F. Guyot, J. Peyronneau, and J.-P. Poirier, High-pressure and high-temperature reactions between silicates and liquid iron alloys in the diamond anvil cell, studied by analytical electron microscopy, *J. Geophys. Res., 97*, 4477-4487, 1992.

Grand, S. P., R. D. van der Hilst, and S. Widiyantoro, Global seismic tomography: A snapshot of convection in the Earth, *GSA Today, 7*, 1-7, 1997.

Gurnis, M., The effects of chemical density differences on convective mixing in the Earth's mantle, *J. Geophys. Res., 91*, 11,407-11,419, 1986.

Gurnis, M., and G. F. Davies, The effect of depth-dependent viscosity on convective mixing in the mantle and the possible survival of primitive mantle, *Geophys. Res. Lett., 13*, 541-544, 1986.

Gutenberg, B., Über die Konstitution des Erdinnern, erschlossen aus Erdbebenbeobachtungen, *Phys. Zeitschrift, 14*, 1217-1218, 1913.

Gutenberg, B., and C. F. Richter, On seismic waves, *Beitr. Geophys., 54*, 94-136, 1939.

Haddon, R. A. W., and J. R. Cleary, Evidence for scattering of seismic *PKP* waves near the core-mantle boundary, *Phys. Earth Planet. Int., 8*, 211-234, 1974.

Hansen, U., and D. A. Yuen, Numerical simulation of thermal chemical instabilities at the core-mantle boundary, *Nature, 334*, 237-240, 1988.

Hansen, U., and D. A. Yuen, Dynamical influences from thermal-chemical instabilities at the core-mantle boundary, *Geophys. Res. Lett., 16*, 629-632, 1989.

Hedlin, M. A. H., P. M. Shearer, and P. S. Earle, Seismic evidence for small-scale heterogeneity throughout the Earth's mantle, *Nature, 387*, 145-150, 1997.

Honda, S., D. A. Yuen, S. Balachandar, and D. Reuteler, Three-dimensional instabilities of mantle convection with multiple phase transitions, *Science, 259*, 1308-1311, 1993.

Houard, S., and H.-C. Nataf, Further evidence for the 'Lay discontinuity' beneath northern Siberia and the North Atlantic from short-period *P*-waves recorded in France, *Phys. Earth Planet. Int., 72*, 264-275, 1992.

Houard, S., and H.-C. Nataf, Laterally varying reflector at the top of D″ beneath northern Siberia, *Geophys. J. Int., 115*, 168-182, 1993.

Husebye, E. S., D. W. King, and R. A. W. Haddon, Precursors to *PKIKP* and seismic wave scattering near the core-mantle boundary, *J. Geophys. Res., 81*, 1870-1882, 1976.

Inoue, H., Y. Fukao, K. Tanabe, and Y. Ogata, Whole mantle *P*-wave travel time tomography, *Phys. Earth Planet. Int., 59*, 294-328, 1990.

Ito, E., E. Takahashi, and Y. Matsui, The mineralogy and chemistry of the lower mantle: an implication of the ultrahigh-pressure phase relations in the system MgO-FeO-SiO_2, *Earth Planet. Sci. Lett., 67*, 238-248, 1984.

Jeanloz, R., Chemical reactions at Earth's core-mantle boundary: Summary of evidence and geomagnetic implications, in *Relating Geophysical Structures and Processes: The Jeffreys Volume, Geophys. Monogr. Ser.*, Vol. 76, edited by K. Aki and R. Dmowska, pp. 121-127, AGU, Washington, D. C., 1993.

Jeffreys, H., The times of P, S, and SKS and the velocities of P and S, *Mon. Not. R. Astron. Soc., 4*, 498-533, 1939.

Kellogg, L. H., Growing the Earth's D″ layer: effect of density variations at the core-mantle boundary, *Geophys. Res. Lett., 24*, 2749-2752, 1997.

Kellogg, L. H., and S. D. King, Effect of mantle plumes on the growth of D″ by reaction between the core and mantle, *Geophys. Res. Lett.*, 20, 379-382, 1993.

Kendall, J. M., and C. Nangini, Lateral variations in D″ below the Caribbean, *Geophys. Res. Lett., 23*, 399-402, 1996.

Kendall, J. M., and P. M. Shearer, Lateral variations in D″ thickness from long-period shear-wave data, *J. Geophys. Res., 99*, 11,575-11,590, 1994.

Kendall, J. M., and P. M. Shearer, On the structure of the lowermost mantle beneath the southwest Pacific, southeast Asia and Australasia, *Phys. Earth Planet. Int., 92*, 85-98, 1995.

Kendall, J. M., and P. G. Silver, Constraints from seismic anisotropy on the nature of the lowermost mantle, *Nature, 381*, 409-412, 1996.

Kennett, B. L. N., E. R. Engdahl, and R. Buland, Constraints on seismic velocities in the Earth from traveltimes, *Geophys. J. Int., 122*, 108-124, 1995.

Kesson, S. E., and J. D. Fitz Gerald, Partitioning of MgO, FeO, NiO, MnO, and Cr_2O_3 between magnesian silicate perovskite and magnesiowüstite: Implications for the origin of inclusions in diamond and the composition of the lower mantle, *Earth Planet. Sci. Lett., 111*, 229-240, 1991.

Kesson, S. E., J. D. Fitz Gerald, and J. M. G. Shelley, Mineral chemistry and density of subducted basaltic crust at lower-mantle pressures, *Nature, 372*, 767-769, 1994.

Knittle, E., and R. Jeanloz, Synthesis and equation of state of *(Mg, Fe)*SiO_3 perovskite to over 100 GPa, *Science, 235*, 668-670, 1987.

Knittle, E., and R. Jeanloz, Simulating the core-mantle boundary: an experimental study of high-pressure reactions between silicates and liquid iron, *Geophys. Res. Lett., 16*, 609-612, 1989.

Knittle, E., and R. Jeanloz, The high pressure phase diagram of $Fe_{0.94}O$: A possible constituent of the Earth's core, *J. Geophys. Res., 96*, 16169-16180, 1991.

Krüger, F., M. Weber, F. Scherbaum, and J. Schlittenhardt, Double beam analysis of anomalies in the core-mantle boundary region, *Geophys. Res. Lett., 20*, 1475-1478, 1993.

Krüger, F., M. Weber, F. Scherbaum, and J. Schlittenhardt, Normal and inhomogeneous lowermost mantle and core-mantle boundary under the Arctic and Northern Canada, *Geophys. J. Int., 122*, 637-658, 1995.

Krüger, F., F. Scherbaum, M..Weber, and J. Schlittenhardt, Analysis of asymmetric multipathing with a generalization of the double beam method, *Bull. Seismol. Soc. Am., 86*, 737-749, 1996.

Kumagai, H., Y. Fukao, N. Suda, and N. Kobayashi, Structure of the D″ layer inferred from the Earth's free oscillations, *Phys. Earth Planet. Inter.*, 73, 38-52, 1992.

Kuo, B. Y., and K. Y. Wu, Global shear velocity heterogeneities in the D″ layer: Inversion from *Sd-SKS* differential travel times, *J. Geophys. Res., 102*, 11775-11788, 1997.

Lavely, E. M., D. W. Forsyth, and P. Friedmann, Scales of heterogeneity near the core-mantle boundary, *Geophys. Res. Lett.*, 13, 1505-1508, 1986.

Lay, T., Structure of the core-mantle transition zone: a chemical and thermal boundary layer, *Eos Trans. AGU, 70*, 49, 54-55, 58-59, 1989.

Lay, T., Seismology of the lowermost mantle and core-mantle boundary, *Rev. of Geophys., Suppl.*, 325-328, 1995.

Lay, T., and D. V. Helmberger, A lower mantle *S*-wave triplication and the velocity structure of D″, *Geophys. J. R. astron. Soc., 75*, 799-837, 1983.

Lay, T., and C. J. Young, Analysis of seismic *SV* waves in the core's penumbra, *Geophys. Res. Lett., 18*, 1373-1376, 1991.

Lay, T., and C. J. Young, Imaging scattering structures in the lower mantle by migration of long-period *S* waves, *J. Geophys. Res., 101*, 20,023-20,040, 1996.

Lay, T., E. J. Garnero, C. J. Young, and J. B. Gaherty, Scale-lengths of shear velocity heterogeneity at the base of the mantle from *S* wave differential travel times, *J. Geophys. Res., 102*, 9887-9910, 1997.

Lay, T., E. J. Garnero, Q. Williams, B. Romanowicz, L. Kellogg, and M. E. Wysession, Seismic wave anisotropy in the D″ region and its implications, in *Observational and Theoretical Constraints on he Core-Mantle Boundary Region*, ed. by M. Gurnis, M. Wysession, B. Buffett and E. Knittle, AGU, Washington, D. C., this volume, 1998.

Li, X. D. and B. Romanowicz, Global mantle shear velocity model developed using nonlinear asymptotic coupling theory, *J. Geophys. Res., 101*, 22245-22272, 1996.

Loper , D. E., and T. Lay, The core-mantle boundary region, *J. Geophys. Res., 100*, 6397-6420, 1995.

Mao, H. K., and P. M. Bell, Equations of state of MgO and epsilon Fe under static pressure conditions, *J. Geophys., Res., 84*, 4533-4536, 1979.

Mao, H. K., C. Chen, R. J. Hemley, A. P. Jephcoat, Y. Wu, and W. A. Bassett, Stability and equation of state of $CaSiO_3$-perovskites to 134 GPa, *J. Geophys. Res., 94*, 17,889-17,894, 1989.

Masters, G., S. Johnson, G. Laske, and H. Bolton, A shear-velocity model of the mantle, *Phil. Trans. R. Soc. Lond. A*, 354, 1385-1411, 1996.

Matzel, Eric, Mrinal K. Sen, and Stephen P. Grand, Evidence for anisotropy in the deep mantle beneath Alaska, Geophys. Res. Lett., 23, 2417-2420, 1996.

Maupin, V., On the possibility of anisotropy in the D" layer as inferred from the polarisation of diffracted *S* waves, *Phys. Earth Planet. Int., 87*, 1-32, 1994.

McCammon, C. A., Perovskite as a possible sink for ferric iron in the lower mantle, Nature, 387, 694-696, 1997.

McCammon, C. A., J. W. Harris, B. Harte, and M. T. Hutchison, Partitioning of ferric iron between lower mantle phases: Results from natural and synthetic samples, *J. Conf. Abstr., 1*, 390, 1996.

McSweeney, T. J., and K. C. Creager, Global core-mantle boundary structure inferred from *PKP* differential travel times, (abstract), *Eos Trans. AGU Supplement, 75*, 663, 1994.

Mitchell, B. J., and D. V. Helmberger, Shear velocities at the base of the mantle from observations of *S* and *ScS*, *J. Geophys. Res., 78*, 6009-6020, 1973.

Nataf, H.-C., and S. Houard, Seismic discontinuity at the top of D": A world-wide feature?, *Geophys. Res. Lett., 20*, 2371-2374, 1993.

Neuberg, J., and J. Wahr, Detailed investigation of a spot on the core-mantle boundary using digital *PcP* data, *Phys. Earth planet. Int., 68*, 132-143, 1991.

O'Mongáin, A., and J. Neuberg, D" topography: Fact or fiction (abstract), *Eos Trans. AGU Supplement, 77*, F679, 1996.

Olivieri, M., N. A. Pino, and A. Morelli, Evidence for an *S*-velocity discontinuity in the lowermost mantle beneath the South Eastern Pacific Basin, *Geophys. Res., Lett., 24*, 2617-2620, 1997.

Olson, P. L., and C. Kincaid, Experiments on the interaction of thermal convection and compositional layering at the base of the mantle, *J. Geophys. Res., 96*, 4347-4354, 1991.

Poirier, J.-P., Core-infiltrated mantle and the nature of the D" layer, *J. Geomagn. Geoelectr., 45*, 1221-1227, 1993.

Pulliam, R. J., D. W. Vasco, and L. R. Johnson, Tomographic inversions for mantle *P* wave velocity structure based on the minimization of l^2 and l^1 norms of International Seismological Centre travel time residuals, *J. Geophys. Res.*, 98, 699-734, 1993.

Revenaugh, J., and T. H. Jordan, Mantle layering from *ScS* Reverberations, 3, The transition zone, *J. Geophys. Res., 96*, 19763-19780, 1991a.

Revenaugh, J., and T. H. Jordan, Mantle layering from *ScS* Reverberations, 4, The lower mantle and core-mantle boundary, *J. Geophys. Res., 96*, 19811-19824, 1991b.

Ricard, Y., M. Richards, C. Lithgow-Bertelloni, and Y. Le Stunff, A geodynamic model of mantle density heterogeneity, *J. Geophys. Res., 98*, 21,895-21,909, 1993.

Richards, P. G., Seismic waves reflected from velocity gradient anomalies within the Earth's upper mantle, *Z. Geophys., 38*, 517-527, 1972.

Richards, M. A. and Davies, G. F., On the separation of relatively buoyant components from subducted lithosphere, *Geophys. Res. Lett., 16*, 831-834, 1989.

Richards, M. A., and D. C. Engebretson, The history of subduction , and large-scale mantle convection, *Nature, 355*, 437-440, 1992.

Rigden, S. M., T. J. Ahrens, E. M. Stolper, Shock compression of molten silicates; results for a model basaltic composition, *J. Geophys. Res., 93*, 367-382, 1988.

Ringwood, A. E., and W. Hibberson, Solubilities of mantle oxides in molten iron at high pressures and temperatures: Implications for the composition and formation of Earth's core, *Earth Planet. Sci. Lett., 102*, 235-251, 1991.

Ritsema, J., E. Garnero, and T. Lay, A strongly negative shear velocity gradient and lateral variability in the lowermost mantle beneath the Pacific, *J. Geophys. Res., 102*, 20,395-20,411, 1997.

Robertson, G. S., and J. H. Woodhouse, Ratio of relative S to P velocity heterogeneity in the lower mantle, *J. Geophys. Res., 101*, 20,041-20,052, 1996.

Ruff, L., and D. L. Anderson, Core formation, evolution, and convection: A geophysical model, *Phys. Earth Planet. Int., 21*, 181-201, 1980.

Schimmel, M., and H. Paulssen, Steeply reflected *ScSH* precursors from the D" region, *J. Geophys. Res., 101*, 16,077-16,088, 1996.

Schlittenhardt, J., Investigation of the velocity- and Q-structure of the lowermost mantle using *PcP/P* amplitude ratios from arrays at distances of 70°-84°, *J. Geophys., 60*, 1-18, 1986.

Scherbaum, F., F. Krüger, and M. Weber, Double beam imaging: Mapping lower mantle heterogeneities using combinations of source and receiver arrays, *J. Geophys. Res., 102*, 507-522, 1997.

Schubert, G., P. Olson, C. A. Anderson, and P. Goldman, Mantle plumes, solitons and the D" layer (abstract), *Eos Trans. AGU, 68*, 1488, 1987.

Shearer, P. M., and T. G. Masters, Global mapping of topography on the 660-km discontinuity, *Nature, 355*, 791-796, 1992.

Sherman, D. M., Equation of state and high-pressure phase transitions of Stishovite (SiO_2): Ab initio (Periodic Hartree-Fock) results, *J. Geophys. Res, 98*, 11,865-11,873, 1993.

Shibutani, T., A. Tanaka, M. Kato, and K. Hirahara, A study of *P*-wave velocity discontinuity in D" layer with J-array records: Preliminary results, *J. Geomag. Geoelectr., 45*, 1275-1285, 1993.

Silver, P. G., R. W. Carlson, and P. Olson, Deep slabs, geochemical heterogeneity, and the large-scale structure of mantle convection: investigation of an enduring paradox, *Ann. Rev. Earth Planet. Sci., 16*, 477-541, 1988.

Sleep, N. H., Gradual entrainment of a chemical layer at the base of the mantle by overlying convection, *Geophys. J. R. astron. Soc., 95*, 437-447, 1988.

Sleep, N. H., Hotspots and mantle plumes: Some phenomenology, *J. Geophys. Res., 95*, 6715-6736, 1990.

Song, X., and D. V. Helmberger, Effect of velocity structure in D" on *PKP* phases, *Geophys. Res. Lett., 20*, 285-288, 1993.

Souriau, A. and G. Poupinet, Lateral variations in *P* velocity and attenuation in the D" layer, from diffracted *P* waves, *Phys. Earth Planet. Int., 84*, 227-234, 1994.

Stacey, F. D., Effects on the core of structure within D", *Geophys. Astrophys. Fluid Dyn., 60*, 157-163, 1991.

Stacey, F. D., and D. E. Loper, The thermal boundary-layer interpretation of D″ and its role as a plume source, *Phys. Earth Planet. Inter.*, *33*, 45-55, 1983.

Steinbach, V. C., D. A. Yuen, G. Y. A. Bussod, H. Paulssen, Effects of depth-dependent properties on the thermal anomalies produced in flush instabilities from phase transitions, *Phys. Earth Planet. Int.*, 86, 165-183, 1994.

Stevenson, D., Infiltration, dissolution and underplating: Rules for mixing core-mantle cocktails (abstract), Eos Trans. AGU, 69, 1404, 1988.

Stevenson, D. J., Why D″ is unlikely to be caused by core-mantle interactions (abstract), *Eos Trans. AGU Supplement, 74*, 51, 1993.

Stixrude, L., and M. S. T. Bukowinski, Stability of (Mg,Fe)SiO_3 perovskite and the structure of the lowermost mantle, *Geophys. Res. Lett.*, *19*, 1057-1060, 1992.

Stixrude, L., R. J. Hemley, Y. Fei, and H. K. Mao, Thermoelasticity of silicate perovskite and magnesiowüstite and stratification of the Earth's mantle, *Science, 257*, 1099-1101, 1992

Su, W., R. L. Woodward, and A. M. Dziewonski, Degree 12 model of shear velocity heterogeneity in the mantle, *J. Geophys. Res.*, *99*, 6945-6981, 1994.

Sylvander, M. and A. Souriau, *P*-velocity structure of the core-mantle boundary region inferred from *PKP(AB)-PKP(BC)* differential travel times, *Geophys. Res. Lett.*, *23*, 853-856, 1996.

Tackley, P. J., D. J. Stevenson, G. A. Glatzmaier, and G. Schubert, Effects of an endothermic phase transition at 670 km depth in a spherical model of convection in the Earth's mantle, *Nature*, *361*, 699-704, 1993.

Tanimoto, T., Long-wavelength *S*-wave velocity structure throughout the mantle, *Geophys. J. Int.*, *100*, 327-336, 1990.

Thomas, C., and M. Weber, P velocity heterogeneities in the lower molten determined with the German regional seismic network: Improvement of previous models and results of 2D modeling, *Phys. Earth Planet. Int.*, *101*, 105-117, 1997.

Tsuchida, Y., and T. Yagi, A new, post-stishovite high-pressure polymorph of silica, *Nature, 340*, 217-220, 1989.

Valenzuela, R. W., and M. E. Wysession, Illuminating the base of the mantle with core-diffracted waves, in *Observational and Theoretical Constraints on he Core-Mantle Boundary Region*, ed. by M. Gurnis, M. Wysession, B. Buffett and E. Knittle, AGU, Washington, D. C., this volume, 1998.

Van der Hilst, R. D., S. Widiyantoro, and E. R. Engdahl, Evidence for deep mantle circulation from global tomography, *Nature*, *386*, 578-584, 1997.

Vasco, D. W., L. R. Johnson, R. J. Pulliam, and P. S. Earle, Robust inversion of IASP91 travel time residuals for mantle *P* and *S* velocity structure, earthquake mislocations, and station corrections, *J. Geophys. Res.*, *99*, 13,727-13,755, 1994.

Vassiliou, M. S., and T. J. Ahrens, The equation of state of $Mg_{0.6}Fe_{0.4}O$ to 200 GPa, *Geophys. Res. Lett.*, *9*, 127-130, 1982.

Vidale, J. E., and H. M. Benz, A sharp and flat section of the core-mantle boundary, *Nature, 359*, 627-629, 1993a.

Vidale, J. E., and H. M. Benz, Seismological mapping of fine structure near the base of the Earth's mantle, *Nature*, *361*, 529-532, 1993b.

Vidale, J. E., and M. A. H. Hedlin, Intense scattering at the core-mantle boundary north of Tonga: Evidence for partial melt, *Nature*, in press, 1998.

Vinnik, L. P., and G. G. Dashkov, *PcP* waves from atomic explosions and the nature of the core-mantle boundary, *Izv., Earth Physics*, *1*, 7-16, 1970.

Vinnik, L., B. Romanowicz, Y. Le Stunff, and L. Makeyeva, Seismic anisotropy in the D″ layer, *Geophys. Res. Lett.*, *22*, 1657-1660, 1995.

Weber, M., *P* and *S* wave reflections from anomalies in the lowermost mantle, *Geophys. J. Int.*, *115*, 183-210, 1993.

Weber, M., Lamellae in D″? An alternative model for lower mantle anomalies, *Geophys. Res. Lett.*, *21*, 2531-2534, 1994.

Weber, M., and J. P. Davis, Evidence of a laterally variable lower mantle structure from P- and S-waves, *Geophys. J. Int.*, *102*, 231-255, 1990.

Weber, M., and M. Körnig, Lower mantle inhomogeneities inferred from *PcP* precursors, *Geophys. Res. Lett.*, *17*, 1993-1996, 1990.

Weber, M., and M. Körnig, A search for anomalies in the lowermost mantle using seismic bulletins, *Phys. Earth Planet. Int.*, *73*, 1-28, 1992.

Weber, M., J. P. Davis, C. Thomas, F. Krüger, F. Scherbaum, J. Schlittenhardt, and M Körnig, The structure of the lowermost mantle as determined from using seismic arrays, in *Seismic Modelling of the Earth's Structure*, Edited by E. Boschi, G Ekström, and A. Morelli, pp. 399-442, Istit. Naz. di Geophys., Rome, 1996.

Weinstein, S. A., Catastrophic overturn in the Earth's mantle driven by multiple phase changes and internal heat generation, *Geophys. Res. Lett.*, *20*, 101-104, 1993.

Wicks, C. W., and M. A. Richards, Seismic evidence for the 1200 km discontinuity (abstract), *Eos Trans. AGU*, *74(43)*, Spring Meeting suppl., 550, 1993.

Williams, Q., and E. J. Garnero, On the possible origin of a seismically thin boundary layer at the base of the mantle, *Science*, *273*, 1528-1530, 1996.

Williams, Q., E. Knittle, and R. Jeanloz, The high-pressure melting curve of iron: A technical discussion, *J. Geophys. Res.*, *96*, 2171-2184, 1991.

Witte, H., Beiträge zur Berechnung der Geschwindigkeit der Raumwellen im Erdinnern, *Nachrichten der Gesellschaft der Wissenschaften zu Göttingen, Heft* 2, pp. 199-241, 1932.

Wood, B. J., and D. C. Rubie, The effect of alumina on phase transformations at the 660-kilometer discontinuity from Fe-Mg partitioning experiments, *Science, 273*, 1522-1524, 1996.

Woodward, R. L., and G. Masters, Lower-mantle structure from *ScS-S* differential travel times, *Nature, 352*, 231-233, 1991.

Wright, C., Array studies of *P* phases and the structure of the D″ region of the mantle, *J. Geophys. Res.*, *78*, 4965-4982, 1973.

Wright, C., and J. A. Lyons, Seismology, dT/dΔ and deep mantle convection, *Geophys. J. R. Astron. Soc.*, *40*, 115-138, 1975.

Wright, C., and J. A. Lyons, Further evidence for radial velocity anomalies in the lower mantle, *Pure Appl. Geophys.*, *119*, 137-162, 1981.

Wright, C., Muirhead, K. J., and A. E. Dixon, The *P* wave velocity structure near the base of the mantle, *J. Geophys. Res.*, *90*, 623-634, 1985.

Wysession, M. E., Large-scale structure at the core-mantle boundary from core-diffracted waves, *Nature*, *382*, 244-248, 1996a.

Wysession, M. E., Imaging cold rock at the base of the mantle: The sometimes fate of Slabs?, in *Subduction: Top to Bottom*, edited by G. E. Bebout, D. Scholl, S. Kirby, and J. P. Platt, AGU, Washington, D. C., pp. 369-384, 1996b.

Wysession, M. E., E. A. Okal and C. R. Bina, The structure of the core-mantle boundary from diffracted waves, *J. Geophys. Res.*, *97*, 8749-8764, 1992.

Wysession, M. E., C. R. Bina and E. A. Okal, Constraints on the temperature and composition of the base of the mantle, in *Dynamics of the Earth's Deep Interior and Earth Rotation, Geophys. Monogr. Ser.*, edited by J.-L. LeMoüel et al., AGU, Washington, D.C., 181-190, 1993.

Wysession, M. E., L. Bartkó, and J. Wilson, Mapping the lowermost mantle using core-reflected shear waves, *J. Geophys. Res.*, *99*, 13,667-13,684, 1994.

Wysession, M. E., S. Robertson, G. I. Al-eqabi, A. Langenhorst, M. J. Fouch, K. M. Fischer, and T. J. Clarke, D" lateral, vertical and anisotropic structure from MOMA core-diffracted waves, *Eos Trans. AGU*, *78*(46), Fall Meeting suppl., F1, 1997.

Yamada, A., and I. Nakanishi, Detection of P wave reflector in D" beneath the southwestern Pacific using double-array stacking, *Geophys. Res. Lett.*, *23*, 1553-1556, 1996.

Young, C. J., and T. Lay, The core mantle boundary, *Ann. Rev. Earth Planet. Sci.*, *15*, 25-46, 1987*a*.

Young, C. J., and T. Lay, Evidence for a shear velocity discontinuity in the lower mantle beneath India and the Indian Ocean, *Phys. Earth Planet. Inter.*, *49*, 37-53, 1987*b*.

Young, C. J., and T. Lay, Multiple phase analysis of the shear velocity structure in the D" region beneath Alaska, *J. Geophys. Res.*, *95*, 17,385-17,402, 1990.

Yuen, D. A., O. P. Cadek, A. Chopelas, and C. Matyska, Geophysical inferences of thermal-chemical structures in the lower mantle, *Geophys. Res. Lett.*, *20*, 899-902, 1993.

Yuen, D. A., O. P. Cadek, R. Boehler, J. Moser, and C. Matyska, Large cold anomalies in the deep mantle and mantle instability in the Cretaceous, *Terra Nova*, *6*, 238-245, 1994.

Zhu, A.-N., and M. E. Wysession, Mapping global D" *P* velocity structure from ISC *PcP-P* differential travel times, *Phys. Earth Planet. Int.*, *99*, 69-82, 1997.

Zhang, S., and D. A. Yuen, Deformation of the core-mantle boundary induced by spherical shell, compressible convection, *Geophys. Res. Lett.*, *14*, 899-902, 1987.

Zhang, S., and D. A. Yuen, Dynamical effects on the core-mantle boundary from depth-dependent thermodynamical properties of the lower mantle, *Geophys. Res. Lett.*, *15*, 451-454, 1988.

Zhao, Y., and D. L. Anderson, Mineral physics constraints on the chemical composition of the Earth's lower mantle, *Phys. Earth Planet. Int.*, *85*, 273-292, 1994.

M. E. Wysession, Department of Earth and Planetary Sciences, Washington University, St. Louis, MO 63130

T. Lay, J. Revenaugh, and Q. Williams, Institute of Tectonics and Earth Sciences Department, University of California, Santa Cruz, CA 95064

E. J. Garneroand R. Jeanloz, Department of Geology and Geophysics, University of California, Berkeley, CA 94720

L. H. Kellogg, Geology Department, University of California, Davis, CA 95616